CaMKII locally encodes L-type channel activity to signal to nuclear CREB in excitation–transcription coupling

Damian G. Wheeler, Curtis F. Barrett, Rachel D. Groth, Parsa Safa, and Richard W. Tsien

Department of Molecular and Cellular Physiology, Stanford University School of Medicine, Stanford, CA 94305

Communication between cell surface proteins and the nucleus is integral to many cellular adaptations. In the case of ion channels in excitable cells, the dynamics of signaling to the nucleus are particularly important because the natural stimulus, surface membrane depolarization, is rapidly pulsatile. To better understand excitation–transcription coupling we characterized the dependence of cAMP response element–binding protein phosphorylation, a critical step in neuronal plasticity, on the level and duration of membrane depolarization. We find that signaling strength is steeply dependent on depolarization, with sensitivity far greater than hitherto recognized. In contrast, graded blockade of the Ca^{2+} channel pore has a remarkably mild effect, although some Ca^{2+} entry is absolutely required. Our data indicate that Ca^{2+}/CaM-dependent protein kinase II acting near the channel couples local Ca^{2+} rises to signal transduction, encoding the frequency of Ca^{2+} channel openings rather than integrated Ca^{2+} flux—a form of digital logic.

Introduction

In excitable cells, voltage-dependent Ca^{2+} channels perform the important task of coupling membrane depolarization to diverse biological responses, including muscle contraction, secretion, and gene expression (Hille, 2001). Much is known about relationships between channel activation and biological output in excitation–contraction (E-C) and excitation–secretion (E-S) coupling. For example, E-C and E-S coupling both occur close to the channel, on a millisecond time scale. Yet, although coupling to muscle contraction and neurotransmitter release share the generic feature of a steeply cooperative relationship between Ca^{2+} channel activation and functional response, their dependence on Ca^{2+} flux differs (for reviews see Schneider, 1994; Schneggenburger and Neher, 2005). Skeletal E-C coupling shows little or no dependence on Ca^{2+} influx (Armstrong et al., 1972; Schneider and Chandler, 1973; Rios and Brum, 1987; Beam and

Franzini-Armstrong, 1997; Franzini-Armstrong and Protasi, 1997), whereas E-S coupling is exquisitely sensitive to the magnitude of Ca^{2+} entry (Dodge and Rahamimoff, 1967; Llinas et al., 1981; Augustine et al., 1985; Bollmann et al., 2000; Schneggenburger and Neher, 2000; Sudhof, 2004).

Unlike E-C and E-S coupling, excitation–transcription (E-T) coupling has not been so quantitatively examined, possibly because Ca^{2+} channel activation and the final event are widely separated spatially, temporally, and methodologically. First, induction of gene transcription often involves local signaling near the plasma membrane, but culminates in responses in the nucleus, up to tens of micrometers away. Second, brief cell depolarization may drive gene expression minutes to hours later. Third, the initiating event in E-T coupling is electrophysiological but the final outcome is a biochemical response, typically studied in populations of cells. In neurons, the most extensively studied example of E-T coupling is signaling to the transcription factor cAMP response element–binding protein (CREB) via phosphorylation at Ser133, which is critical for CRE-mediated gene expression and many adaptive changes in neurons (Lonze and Ginty, 2002; Carlezon et al., 2005). L-type

The Rockefeller University Press $30.00
J. Cell Biol. Vol. 183 No. 5 849–863
www.jcb.org/cgi/doi/10.1083/jcb.200805048

JCB 849

Ca^{2+} channels play an advantaged role in such signaling (Murphy et al., 1991; West et al., 2002; Deisseroth et al., 2003; Dolmetsch, 2003). The advantage arises because L-type channels have private access to local Ca^{2+}-dependent signaling machinery (Deisseroth et al., 1996; Dolmetsch et al., 2001; Weick et al., 2003; Zhang et al., 2005). Thus, key initial events in E-T coupling may occur near the channel, just as in E-C and E-S coupling.

Considerable uncertainty surrounds functional and molecular aspects of downstream events that mediate signaling from activated L-type channels to the nucleus. CaM basally tethered to L-type channels (Zuhlke et al., 1999) seems essential for MAPK signaling to CREB in response to prolonged depolarization (Dolmetsch et al., 2001). However, whether L-type channels enlist this resident CaM to signal to CREB after brief depolarization is unclear, as are the nature of rapid coupling between depolarization and CREB phosphorylation and the identity of downstream molecular mechanisms.

In addressing unanswered questions, it is worthwhile to note classical studies on E-C and E-S coupling, some dating back half a century (Hodgkin and Horowicz, 1960; Katz and Miledi, 1967; Armstrong et al., 1972; Chapman and Tunstall, 1981; Llinas et al., 1981; Augustine et al., 1985; for reviews see Schneider, 1994; Augustine, 2001; Schneggenburger and Neher, 2005). Such studies addressed generic questions that remain for E-T coupling. How local are the signaling events immediately downstream of Ca^{2+} channel activation? How rapidly is the biochemical sensor engaged? What is the stimulus-response input–output relationship? How steeply does the coupling depend on depolarization, channel gating, and Ca^{2+} influx? We approached these fundamental issues using a method to assess signaling strength in terms of the dynamics of the Ser^{133}-phospho-CREB (pCREB) response. Our findings revealed that E-T coupling depends on Ca^{2+} channel activation in a steeply cooperative manner, following a nearly cubic power law, so that small voltage changes produce large changes in signal strength. This steepness arises from changes in L-type channel open probability (P_o), not simply total Ca^{2+} influx per se, indicating that incoming Ca^{2+} drives a local sensor to near saturation. Several lines of evidence implicated Ca^{2+}/CaM-dependent protein kinase II (CaMKII) as the integrator of channel activity that signals to CREB. Like CREB phosphorylation, local CaMKII activity requires L-type channel gating, yet is only mildly dependent on the magnitude of Ca^{2+} flux. This coupling mechanism provides a form of digital logic wherein depolarizations leading to CREB phosphorylation are encoded in the frequency of Ca^{2+} channel openings rather than the integrated Ca^{2+} flux.

Results

Signaling to nuclear CREB in rat superior cervical ganglion (SCG) neurons

Rat SCG cultures are widely used to study many aspects of neuronal function, including Ca^{2+} channel properties and intracellular Ca^{2+} dynamics (Adams and Brown, 1973; Mains and Patterson, 1973; Hille, 1994). We previously found that depolarizing SCG neurons results in L-type Ca^{2+} channel–dependent phosphorylation of CREB and CRE-mediated gene expression

(Wheeler and Cooper, 2001; Wheeler et al., 2006). Because SCG cultures contain a homogenous population of neurons that do not form functional synapses (O'Lague et al., 1978), raising extracellular $[K^+]$ produces a stable and reproducible depolarization (Wheeler et al., 2006), in essence providing a high-throughput voltage clamp. Thus, we could relate biochemical responses (signaling to nuclear CREB), averaged over many neurons, with electrophysiological and Ca^{2+} imaging measurements obtained from individual neurons.

Basic features of signaling in SCG neurons are illustrated in Fig. 1 (A and B). Depolarization with 40 mM K^+ for 3 min led to nuclear pCREB in every neuron (Fig. 1 B). This signaling required Ca^{2+} influx, as it was not seen with a Ca^{2+}-free solution or after preloading with the Ca^{2+} chelator BAPTA (Fig. 1 A). The L-type channel antagonist nimodipine blocked signaling to CREB (Fig. 1 A), and signaling was rescued by adenoviral-mediated gene transfer of a nimodipine-insensitive L-type channel (Fig. 1 B). FPL 64176, which specifically increases the P_o of L-type channels (Kunze and Rampe, 1992; Liu et al., 2003) drove signaling even in the absence of depolarization (i.e., in 5 mM K^+), consistent with the idea that signaling to CREB is highly sensitive to activation of L-type channels. CREB phosphorylation by 40 mM K^+ was unaffected by blocking Ca_V2 (N and P/Q type) channels (unpublished data), the majority class in SCG neurons (Hirning et al., 1988). With regard to biochemical pathways, the Ca^{2+}/CaM-dependent kinase (CaMK) inhibitor KN93 (but not its inactive congener KN92) blocked signaling, whereas inhibitors of MEK, PKA, and PKC (U0126, KT5720, and bis-indolylmaleimide I, respectively) were without effect (Fig. 1 A).

With respect to Ca^{2+} channel flux, CREB phosphorylation was only mildly reduced by the Ca^{2+} flux inhibitors La^{3+} (200 μM, P < 0.01) and Cd^{2+} (200 μM, P < 0.05), despite blocking the majority of Ca^{2+} current. Further, reducing external Ca^{2+} to 100 μM failed to decrease the pCREB response (P > 0.9). However, when combined, Cd^{2+} and low Ca^{2+} dramatically reduced signaling (P < 0.005), which is consistent with competition between Ca^{2+} and Cd^{2+} for a high affinity pore binding site (Lansman et al., 1986; Chow, 1991; Yang et al., 1993; Ellinor et al., 1995). These data pointed toward an unexpected conclusion: although some Ca^{2+} flux is absolutely required for signaling, large reduction in Ca^{2+} entry only marginally affects signaling. These experiments focused on the steady-state response of pCREB after a prolonged stimulation. To gain insight into underlying mechanisms, we redirected our experiments to focus on the dynamics of signaling.

The relationship between pCREB and stimulus time as a readout of signal strength

Much as monitoring the rate of a biochemical reaction provides an index of enzymatic activity, tracking the development of pCREB provides a measure of relative signal strength in response to a given depolarization. We found that varying stimulation time resulted in graded levels of pCREB. Stimulation with 40 mM K^+ for a few seconds, followed by an appropriate delay, resulted in a weak but clearly detectable pCREB signal in individual neurons (Fig. 1, C and D; and Fig. S1, available
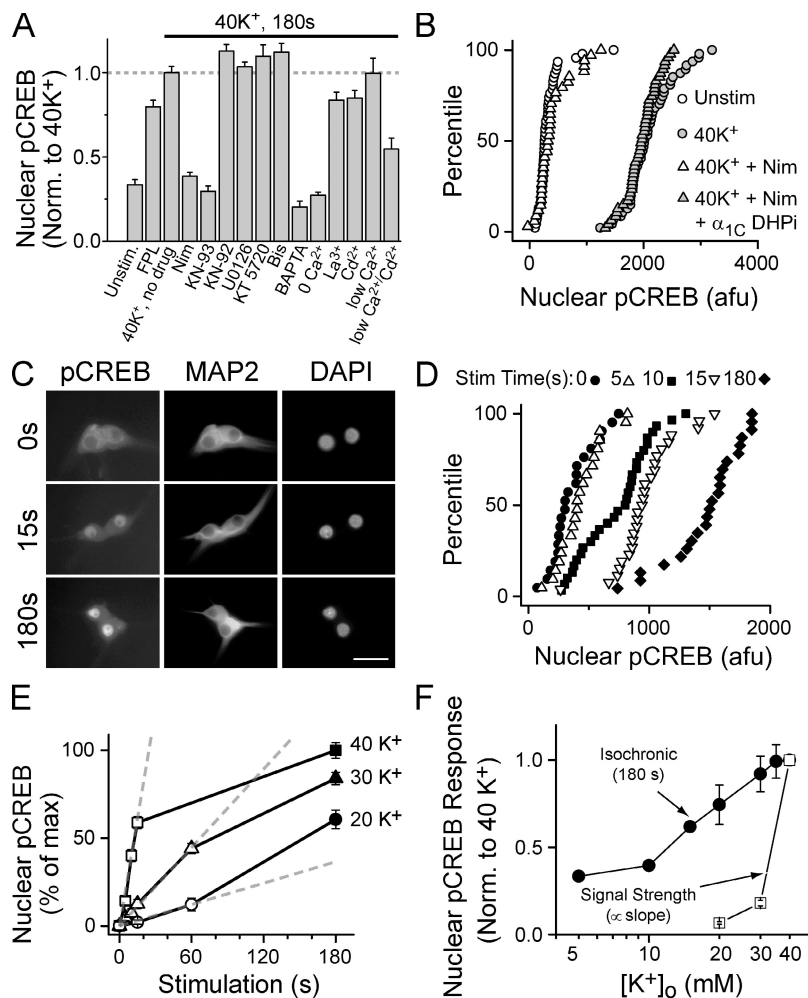
Figure 1. **Strength of signaling to CREB in SCG neurons: dependence on activation of L-type Ca²⁺ channels and a CaM kinase pathway.** (A) Nuclear pCREB levels after a 3-min, 40-mM K⁺ or FPL 64176 stimulation. Drugs (KN-93, CaMK inhibitor; KN-92, inactive congener of KN-93; U0126, MEK inhibitor; KT 5720, PKA inhibitor; Bis [bis-indolylmaleimide I], PKC inhibitor) were added 1 min before stimulation. Some cultures were preloaded with 100 μM BAPTA-AM for 30 min at 37°C, stimulated in 0 mM of extracellular Ca²⁺ and EGTA (0 Ca²⁺) or 100 μM Ca²⁺ and no EGTA (low Ca²⁺), and/or stimulated in 200 μM La³⁺ or Cd²⁺ after preincubation for 1 s. Data are from two or more experiments of >40 neurons each. (B) Cumulative histograms of pCREB levels in individual neurons from a representative experiment. Cells stimulated for 3 min as indicated. Infecting cells with adenovirus expressing dihydropyridine-insensitive L-type Ca²⁺ channel (DHPi) rescued signaling to CREB. (C–E) Data from a representative experiment. Cells were either mock stimulated in 5-mM K⁺ Tyrode's (t = 0) or stimulated with solutions containing 20, 30, or 40 mM K⁺ for the time indicated, placed back in 5 mM K⁺ solution, and then fixed at 3 min. (C) 5–d in vitro SCG neurons stained for pCREB and MAP2; nuclei counterstained with DAPI. Bar, 50 μm. (D) Cumulative histograms of pCREB levels from individual neurons. (E) Mean pCREB levels plotted against stimulation time; [K⁺] as indicated. Dashed lines are linear fits of initial data points; slope used as index of CREB signal strength. (F) Isochronic nuclear pCREB levels measured at 3 min (●); CREB signal strength (□), measured as in E. Isochronic data from three independent experiments, except the 10- and 15-mM K⁺ data are the mean of >15 cells from a single duplicate experiment. Error bars represent SEM.

at http://www.jcb.org/cgi/content/full/jcb.200805048/DC1; see Materials and methods); however, stimulation for 10 s or more largely saturated the pCREB response. In contrast, weaker stimuli (e.g., 20–30 mM K⁺) drove much slower signaling, although pCREB eventually approached the level attained with 40 mM K⁺ (Fig. 1 E). To estimate the strength of signaling, we determined the per-unit-time effect of a given stimulus by measuring the initial slope of the time-dependent increase in pCREB (Fig. 1 E, dashed gray lines). Defined in this way, CREB signal strength was a steep function of external [K⁺] (Fig. 1 F, open squares). Because of rapid saturation, measuring isochronic pCREB levels generated by prolonged depolarization (e.g., 3 min; Fig. 1 F, closed circles) did not reflect the true signaling strength. In contrast, tracking the initial slope of the increase in pCREB revealed a very dramatic change in output with small gradations in input, demonstrating the inherent sensitivity of the signaling system.

CREB signal strength is a steep function of membrane potential and Ca²⁺ channel function

Because CREB signaling was steeply dependent on [K⁺], we related signal strength to both depolarization and channel activity. We measured membrane voltage in various K⁺ concentrations, using external solutions identical to those in the pCREB experiments.

The resting potential in 5 mM K⁺ was approximately –60 mV (Fig. 2, A and B), which is consistent with previous studies (O'Lague et al., 1974; Wheeler et al., 2006). Exposure to 20, 30, and 40 mM K⁺ depolarized the cells to –37, –26, and –19 mV, respectively, following the Nernst relationship (Fig. 2 B). Plotting CREB signal strength against voltage (Fig. 2 C) revealed a steep relationship of 5.6 mV per e-fold change.

To relate CREB signal strength to channel activity, we measured Ca²⁺ currents in 2 mM Ca²⁺, at voltages corresponding to each particular [K⁺]. The mild depolarizations to the voltages indicated in Fig. 2 D elicited small but resolvable Ca²⁺ currents with very little inactivation. Over the voltage range we examined (−37 to −19 mV), Ca²⁺ flux essentially follows the foot of a Boltzmann curve. Accordingly, Ca²⁺ flux displayed an exponential dependence on depolarization (Fig. 2 E), with an e-fold increase per 24.0 mV. This is milder than expected for a single species of Ca²⁺ channel, likely reflecting contributions of multiple L-type channels, including $Ca_V1.3$ (α_{1D}) (Lin et al., 1996), which activates at more negative potentials than $Ca_V1.2$ (α_{1C}) (Xu and Lipscombe, 2001).

Ca²⁺ channel P_o controls CREB signal strength

To examine further the relationship between CREB signal strength and channel activity, we plotted signal strength against
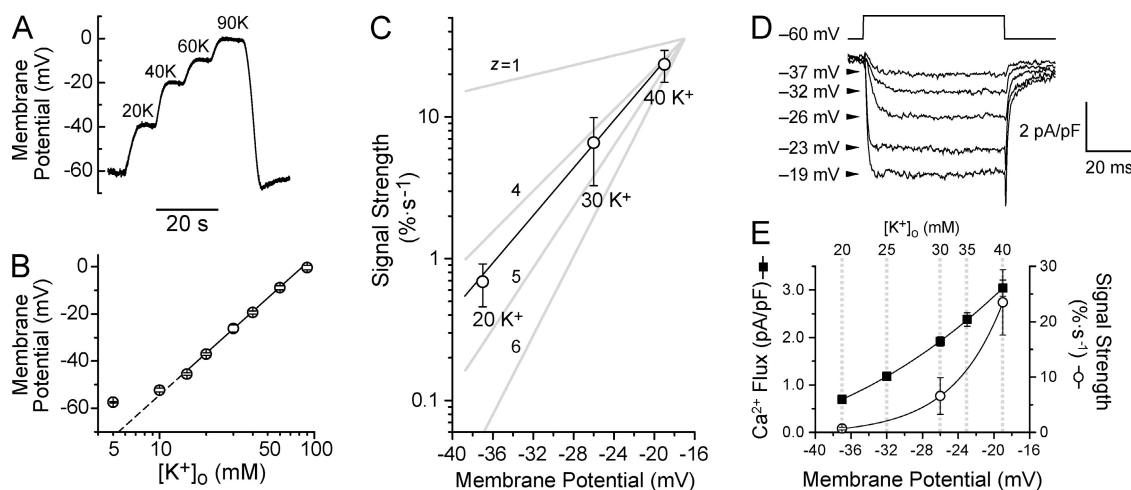
Figure 2. **CREB signal strength is a steep function of membrane potential and channel activity.** (A) SCG neuron under current clamp in TTX. In 4 mM K$^+$, the cell rested at −60 mV. Exposure to [K$^+$]$_o$ as indicated caused stepwise depolarizations. (B) Membrane potential plotted against [K$^+$]$_o$. Slope of linear fit is 58.1 mV per 10-fold change in [K$^+$]$_o$. (C) CREB signal strength, measured as in Fig. 1 E and in Materials and methods (five to eight experiments), plotted against voltage. 100% is the full change in pCREB from baseline to maximal levels. Linear fit shows that signal strength is steeply voltage dependent, as if governed by a gating particle with valence (z) between 4 and 5. (D) Voltage-clamp recordings with 2-mM Ca^{2+} Tyrode's as bathing solution. Pulse depolarizations to the voltages indicated. Traces are the mean of ten consecutive sweeps at each voltage. (E) Ca^{2+} flux (■; as in D) and signal strength (○) plotted versus membrane potential. Solid lines are single exponential fits. Dashed lines indicate the voltages generated by each [K$^+$]$_o$ ($n = 5$–8 experiments). Error bars represent SEM.

total Ca^{2+} flux for stimulations with 20, 30, and 40 mM K$^+$ (Fig. 3 A). On a log–log scale, the data were fit by a straight line with a slope of 2.37, indicating that CREB signal strength was proportional to [Ca^{2+} flux]$^{2.37}$. When CREB signal strength was plotted against the nimodipine-sensitive portion of the flux, the steep relationship remained (Fig. S2, available at http://www.jcb.org/cgi/content/full/jcb.200805048/DC1), confirming that signal strength is steeply dependent on changes in L-type channel activity. The integrated Ca^{2+} flux through an individual channel is the product of channel P_o and unitary Ca^{2+} flux (i_{Ca}). Voltage changes in the range we studied (−37 to −19 mV) will have little effect on i_{Ca}; thus, P_o underlies the steeply increasing signal strength. However, the question remained whether signal strength is determined simply by total Ca^{2+} flux by itself or by underlying changes in channel gating.

Unlike depolarization, which acts on P_o, Cd^{2+} affects i_{Ca}. In Ca^{2+}, Cd^{2+} blocks and unblocks the channel pore on a microsecond scale, thereby decreasing integrated Ca^{2+} flux through

the open channel (Lansman et al., 1986; Chow, 1991). This property is shared by high voltage–activated Ca^{2+} channels such as L- and N-type channels (Wakamori et al., 1998; Sather and McCleskey, 2003), which are the main Ca^{2+} channels expressed in cultured SCG neurons (Hirning et al., 1988). Cd^{2+} potently blocked whole-cell Ca^{2+} flux at −19 mV (Fig. 3 B) without affecting depolarization (unpublished data). We measured signaling to CREB in response to 40 mM K$^+$ (−19 mV) with or without Cd^{2+} (added 1 s before stimulation and maintained throughout). Despite sharply reducing Ca^{2+} flux, Cd^{2+} had a surprisingly mild effect on CREB signal strength (Fig. 3 C); the regression line had a slope of 0.74, much shallower than the slope of 2.37 found for gradations in [K$^+$]. This disparity is underscored by considering stimulation with 40 mM K$^+$ in 200 μM Cd^{2+}, which resulted in much less Ca^{2+} flux than stimulation with 20 mM K$^+$ (P < 10$^{−7}$), yet drove much stronger signaling (P < 0.005). Thus, the trickle of Ca^{2+} flux that remains in the presence of Cd^{2+} is sufficient to engage signaling to CREB.

Figure 3. **CREB signal strength is steeply dependent on channel P_o but not Ca^{2+} flux per se.** (A) Log–log plot of signal strength versus Ca^{2+} flux for the [K$^+$]$_o$ indicated. Solid line shows the linear fit of the data. (B) Whole-cell Ca^{2+} flux (as in Fig. 2 D), in the presence of 0, 20, or 200 μM Cd^{2+}. (C) CREB signal strength for 40 K$^+$ with 0, 20, or 200 μM Cd^{2+} measured as described in Fig. 1 and Materials and methods; $n = 3$–6 experiments. The solid line is a linear fit of the Cd^{2+} data. For comparison, the dashed line and gray data points are reproduced from A. Error bars represent SEM.

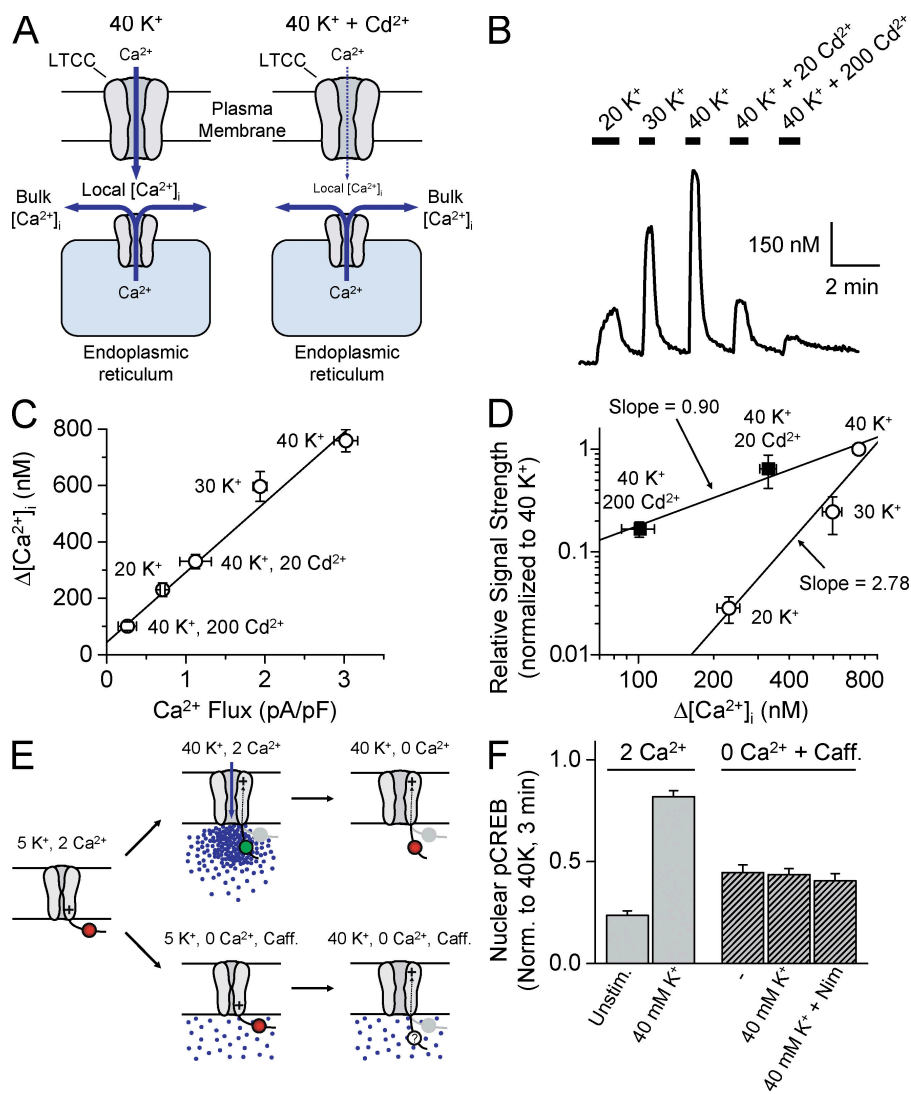**Figure 4. Bulk $[Ca^{2+}]_i$ is neither necessary nor sufficient to dictate CREB signal strength.** (A) Despite Cd^{2+} effects on Ca^{2+} flux, release from intracellular stores might maintain bulk $[Ca^{2+}]$. (B) Fura-2 Ca^{2+} imaging experiment. Various $[K^+]_o$ with and without Cd^{2+} were applied as indicated. (C) Increased $[Ca^{2+}]_i$ plotted against Ca^{2+} flux (from Fig. 3). $\Delta[Ca^{2+}]_i$ data from 10–23 cells and three to five experiments. Linear fit correlation coefficient equals 0.995 (P < 0.0005). (D) Log–log plot of CREB signal strength versus $\Delta[Ca^{2+}]_i$ for the indicated conditions. Solid lines are linear fits through the data points collected with varying $[K^+]_o$ or $[Cd^{2+}]$. (E) Possible gating-driven conformational changes working in concert with elevated bulk Ca^{2+}. (top) Hypothetical conformational change repositions a local signaling determinant (circle). When combined with high local Ca^{2+} elevations, strong signaling to the nucleus is engaged (green). In the Ca^{2+}-free solution (0 Ca^{2+}), the conformational change remains, but the signaling determinant is not activated (red). (bottom) Can conformational change contribute to signaling in conjunction with increases in bulk Ca^{2+}. (F) Nuclear pCREB levels from cells stimulated for 10 s in 2 mM Ca^{2+} (high local Ca^{2+}) or for 15 s in the presence of caffeine with 0 Ca^{2+} (bulk Ca^{2+}). Error bars represent SEM.

In contrast, when L-type channels were completely prevented from opening with nimodipine, signaling to CREB was virtually eliminated (Fig. 1 A). Together, these findings demonstrate that the relationship between depolarization and CREB signal strength is not a simple function of total Ca^{2+} flux, but is closely tied to voltage-dependent changes in P_o.

We also manipulated i_{Ca} by lowering $[Ca^{2+}]_o$ and obtained data similar to the Cd^{2+} results (Fig. 1 A). However, we consider the Cd^{2+} experiments to be more reliable because changing $[Ca^{2+}]_o$ alters membrane surface potential (Hille, 2001) and evokes signaling through the Ca^{2+}-sensing receptor (Vizard et al., 2008), effects that could complicate the interpretation.

Bulk intracellular $[Ca^{2+}]$ does not control signal strength

The steep dependence of signaling on P_o but not i_{Ca} led us to examine how CREB signaling could be highly sensitive to the activation state of the channel, but not the size of the Ca^{2+} flux. An obvious candidate mechanism is conformational coupling between L-type Ca^{2+} channels and ryanodine receptors (RyRs), as in skeletal muscle E-C coupling (Beam and Franzini-

Armstrong, 1997; Franzini-Armstrong and Protasi, 1997; De Crescenzo et al., 2006; for review see Schneider, 1994). However, the requirement for extracellular Ca^{2+} (Fig. 1 A) ruled out a strictly skeletal-like mechanism. In addition, blocking Ca^{2+}-induced Ca^{2+} release from RyRs, a key step in cardiac E-C coupling (Stern, 1992; Cannell et al., 1995; Lopez-Lopez et al., 1995; Guatimosim et al., 2002; Bers and Guo, 2005), did not affect signaling to CREB (Fig. S3, available at http://www.jcb .org/cgi/content/full/jcb.200805048/DC1).

We next considered other mechanisms of Ca^{2+} release from internal stores, e.g., IP$_3$-mediated Ca^{2+} release (Berridge, 1998). For example, a rise in local Ca^{2+} in the narrow space between the plasma membrane and the store membrane (Henkart, 1980; Lencesova et al., 2004) can trigger Ca^{2+} release from stores to elevate bulk $[Ca^{2+}]_i$ (Cannell et al., 1995; Lopez-Lopez et al., 1995; Wang et al., 2001; Guatimosim et al., 2002). In this scenario, even if Ca^{2+} flux were reduced with Cd^{2+}, the local Ca^{2+} rise might still trigger Ca^{2+} release from stores, and signal strength would simply be a function of bulk $[Ca^{2+}]_i$ (Fig. 4 A).

We measured the relationship between signal strength and bulk $[Ca^{2+}]_i$ elevations (measured with the Ca^{2+} indicator Fura-2;

Figure 5. L-type channel activity produces phosphoCaMKII puncta near the cell surface. (A) SCG neurons stimulated with 40 mM K+ for 0, 10, or 60 s and immediately fixed and stained for Map2 (red) and pCaMKII (green). Arrows point to pCaMKII puncta (magnified in the inset). Background pCaMKII staining was subtracted to highlight punctate staining (see Materials and methods). Bar, 20 μm (B) pCaMKII puncta weight from experiments as in A. (C) Nimodipine blocks pCaMKII puncta formation. (D) pCaMKII puncta weight from cells treated for 60 s as shown on a log–log plot against the rise in bulk Ca^{2+} ($\Delta[Ca^{2+}]_i$ are taken from Fig. 4). For all, $n = 3$ independent experiments. Error bars represent SEM.
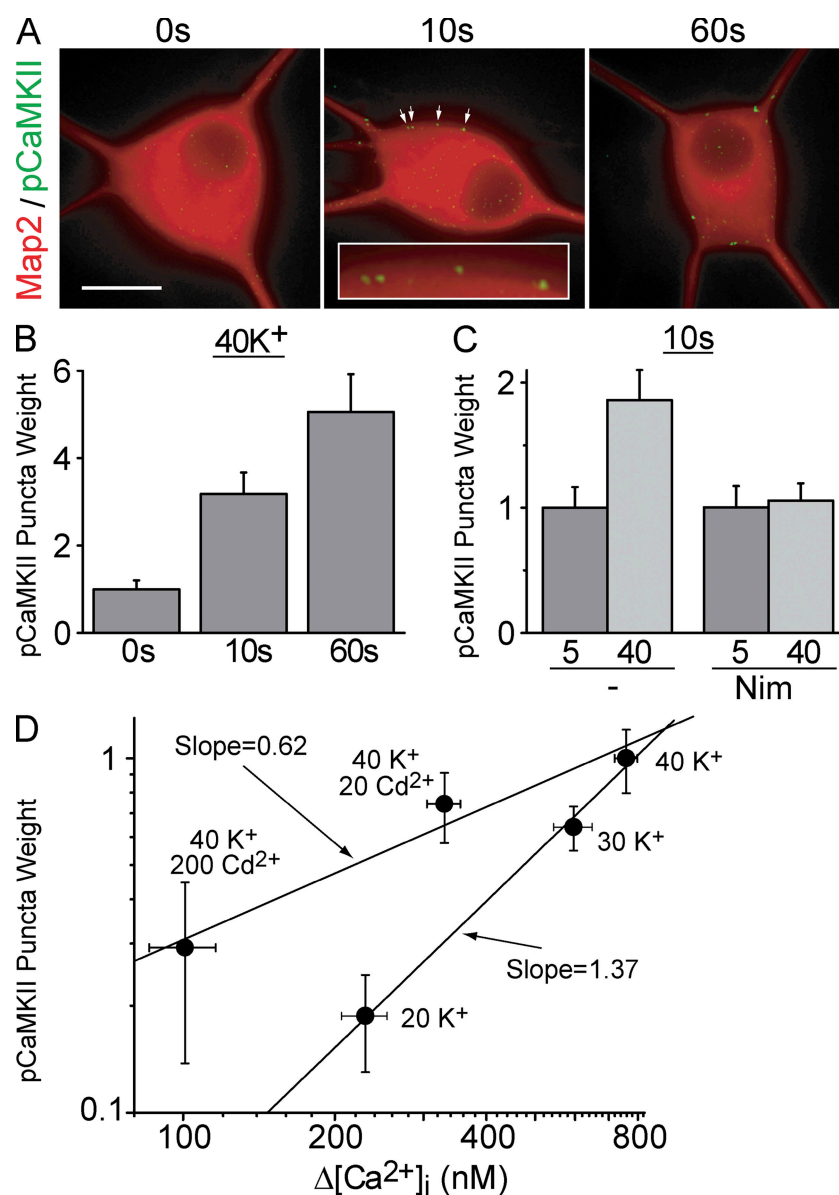
Fig. 4 B). We found a linear relationship between $[Ca^{2+}]_i$ rises and membrane Ca^{2+} flux (Fig. 4 C). Accordingly, when signal strength was plotted against the $[Ca^{2+}]_i$ rise, we observed two distinct relationships (Fig. 4 D), with an approximately threefold difference in slopes on a log–log plot, very similar to disparate relationships we observed with Ca^{2+} flux. Thus, CREB signal strength cannot be solely determined by changes in bulk $[Ca^{2+}]_i$.

As an additional check of the mild dependence on i_{Ca}, we performed similar experiments with La^{3+}, which has long been used to reduce open channel flux (Hagiwara and Takahashi, 1967; Lansman et al., 1986). Like Cd^{2+}, La^{3+} potently blocked the Ca^{2+} rise but had little effect on signal strength (Fig. S4, available at http://www.jcb.org/cgi/content/full/jcb.200805048/DC1).

CREB signal strength is determined by Ca^{2+} acting near the channel

Our results indicated that bulk $[Ca^{2+}]_i$ is not sufficient to determine signal strength. However, $[Ca^{2+}]_i$ may be necessary, sig-

naling in conjunction with L-type channels that act as voltage detectors independent of ion flux (Murata et al., 2005; Hegle et al., 2006; Kaczmarek, 2006). A joint requirement for elevated $[Ca^{2+}]_i$ and L-type channel conformational change would neatly explain both the privileged role of L-type channels and the steep dependence on P_o.

To test this, we independently manipulated $[Ca^{2+}]_i$ and L-type channel conformation (Fig. 4 E). 10 mM caffeine raised $[Ca^{2+}]_i$ by ~250 nM (Fig. S2); this rise was greater than achieved with 40 mM K+/200 μM Cd^{2+}, which produced robust signaling to CREB (Fig. 4 D). In principle, such a rise in $[Ca^{2+}]_i$ meets the putative requirement for bulk Ca^{2+} elevation; indeed, caffeine produced a modest phosphorylation of CREB, even in Ca^{2+}-free solution (Fig. 4 F). In the key test, we looked for an additional effect of a conformational change, produced by depolarizing with a 40-mM K+, Ca^{2+}-free solution. Under these conditions, either with or without nimodipine to block channel gating, depolarization was without additional effect beyond caffeine alone (Fig. 4 F).
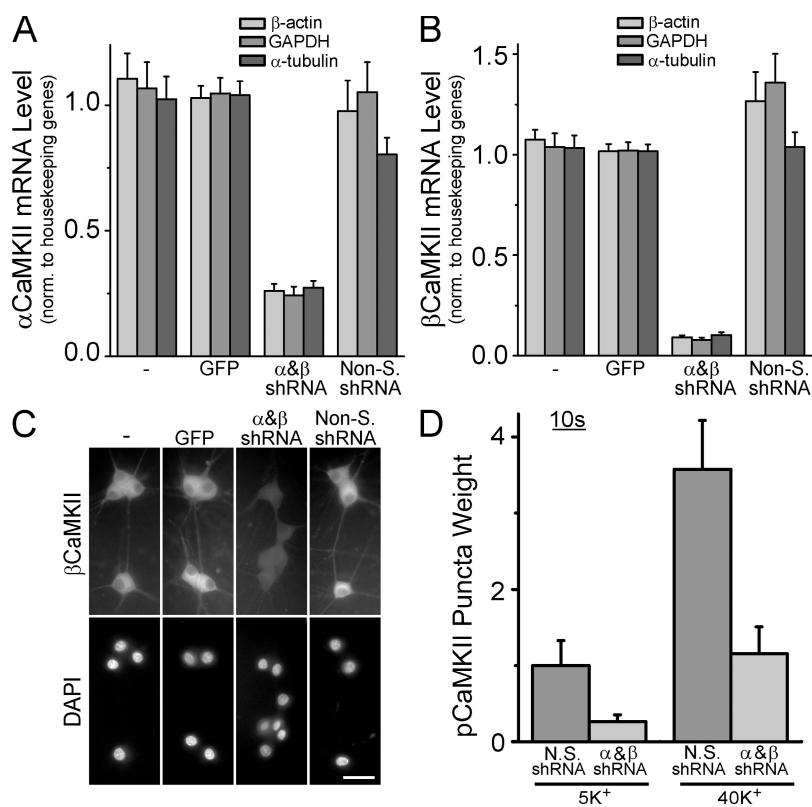
Figure 6. **Knockdown of α and βCaMKII eliminates the formation of pCaMKII puncta.** αCaMKII (A) and βCaMKII (B) mRNA levels in SCG neurons assessed by quantitative RT-PCR. Some cultures infected with lentiviruses expressing GFP alone, shRNAs against α and βCaMKII, or nonsilencing control shRNAs. Data normalized against three housekeeping genes and plotted relative to the GFP only (empty vector) control (see Materials and methods). n = 3–4 experiments done in triplicate. (C) SCG neurons infected as in A and B and stained with an antibody against βCaMKII; nuclei were counterstained with DAPI. Bar, 50 μm. (D) pCaMKII puncta weight from cells infected with α and βCaMKII or nonsilencing control lentiviruses, stimulated for 10 s with 40 mM K$^+$ and immediately fixed. Data from two independent experiments done in duplicate (10–15 neurons each). Error bars represent SEM.

In contrast, Ca^{2+} delivered by surface membrane influx evoked a strong pCREB response (Fig. 4 F, left). These results indicate that pairing voltage-dependent conformational changes with rises in bulk [Ca^{2+}] failed to enhance signaling to CREB. Thus, bulk Ca^{2+} is neither necessary nor sufficient to control CREB signal strength in response to mild depolarization.

CaMKII autophosphorylation at the cell surface correlates with CREB signal strength

Our findings suggested that signaling is mediated by a local Ca^{2+} sensor that is weakly sensitive to changes in i_{Ca} yet highly sensitive to channel P_o. Because closed dwell time (but not open dwell time) is strongly voltage dependent, depolarization changes the channel's duty cycle by increasing the frequency of channel openings and that of transient [Ca^{2+}]$_i$ rises near the channel. Thus, a plausible candidate sensor could be positioned close to L-type channels and responsive to the frequency of local [Ca^{2+}]$_i$ elevations. This led us to consider CaMKII. Although not generally considered important in signaling to CREB (but see Takeda et al., 2007), it is a logical candidate. Because CaMKII is tethered to L-type channels (Hudmon et al., 2005), it is strategically positioned to respond to local [Ca^{2+}]$_i$ transients. Furthermore, autophosphorylation and persistent activation of CaMKII increase steeply with the frequency of Ca^{2+} pulses (De Koninck and Schulman, 1998).

We first asked whether the same stimuli that drive rapid signaling to CREB can activate CaMKII. Brief exposure to 40 mM K$^+$, followed by immediate fixation, resulted in the formation of pCaMKII immunoreactive puncta near the cell surface

(Fig. 5 A), which is consistent with local CaMKII activation. To quantify the extent of activation, we identified pCaMKII puncta by an objective criterion (see Materials and methods) and determined their integrated puncta weight for individual cells. CaMKII activation was rapid, with detectable pCaMKII puncta after a 2.5-s stimulation (not depicted), and increasingly stronger activation at 10 and 60 s (Fig. 5, A and B). As with signaling to CREB, pCaMKII puncta formation required L-type channel activity (Fig. 5 C). Importantly, grading i_{Ca} had a much milder effect on CaMKII activation than changing P_o (Fig. 5 D): the ratio of log–log slopes was 2–3, highly reminiscent of signaling to pCREB itself (compare with Fig. 3 C and Fig. 4 D). Together, these data support the hypothesis that local changes in CaMKII activation help couple L-type channel activation to the nuclear response.

CaMKII is essential for L-type channel signaling to CREB

To directly test the role of CaMKII in signaling to CREB, we knocked down the expression of CaMKII using lentiviruses expressing short hairpin RNAs (shRNAs) targeting both α and βCaMKII, the main CaMKII isoforms in neurons. Knocking down α or β individually resulted in reciprocal mRNA regulation (unpublished data), as previously shown at the protein level (Thiagarajan et al., 2002). Therefore, we knocked down both subunits concurrently and obtained a 75 and 90% decrease in α and βCaMKII mRNA, respectively (Fig. 6, A and B). This reduction was relative to neurons that were uninfected or infected with viruses expressing GFP alone or a nonsilencing shRNA. We verified knockdown at the protein level by immunostaining
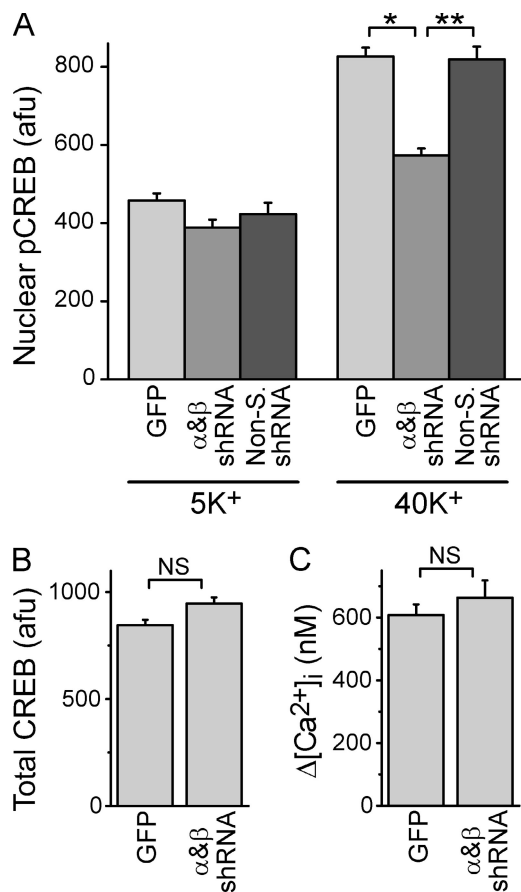
Figure 7. **Knockdown of α and βCaMKII inhibits L-type channel signaling to CREB.** (A) pCREB levels from neurons stimulated for 2.5 s with 5- or 40-mM K^+ Tyrode's and transferred to a 5 mM K^+ solution for 45 s before fixation. Cultures were infected with GFP alone, α and βCaMKII, or non-silencing lentiviruses. Data are from three to six independent experiments (15–30 cells from duplicate coverslips in each). *, $P < 5 \times 10^{-17}$; **, $P < 5 \times 10^{-10}$. (B) Total nuclear CREB levels in neurons infected with GFP alone or α and βCaMKII lentiviruses. Data from three independent experiments, two done in parallel with pCREB experiments in A (46–87 neurons). (C) Peak Ca^{2+} elevations ($\Delta[Ca^{2+}]_i$) from sister cultures to those in B. Data are from seven separate experiments (31–49 cells). Error bars represent SEM.

βCaMKII (Fig. 6 C; the β isoform was chosen because of its robust staining compared with α). Importantly, CaMKII knockdown dramatically reduced pCaMKII puncta formation upon K^+ stimulation (Fig. 6 D).

To test whether CaMKII linked L-type channel activity to CREB signaling, we examined pCREB formation after CaMKII knockdown; to avoid saturating the pCREB response, cells were stimulated with 40 mM K^+ for 2.5 s. When we knocked down both α and βCaMKII, signaling to the nucleus was reduced by >65% (Fig. 7 A), despite normal CREB protein levels (Fig. 7 B) and L-type channel function (Fig. 7 C). Collectively, these data indicated that CaMKII acts downstream of channel activation and Ca^{2+} influx to couple L-type channels to rapid nuclear pCREB formation.

Discussion

E-T coupling is important for a wide range of excitable cells. However, unlike other forms of excitation–response coupling,

many features of E-T coupling have remained unclear. We characterized the basic properties of E-T coupling by relating L-type Ca^{2+} channel activity to the strength of signaling to CREB. We found that signal strength is steeply dependent on Ca^{2+} channel activity, obeying a nearly third power relationship, such that small changes in voltage produced large changes in the nucleus. Surprisingly, when we kept voltage fixed and manipulated Ca^{2+} entry by grading single channel flux, the relationship between Ca^{2+} current and CREB signal strength was far shallower, with an exponent less than one. This dichotomy underscores the conclusion that L-type channel signaling to CREB is not simply dictated by global $[Ca^{2+}]_i$, nor by integrated Ca^{2+} flux, but is responsive to the pattern of channel opening and closing. We hypothesized that Ca^{2+} entry via L-type channels drives a local sensor to saturation, thereby dampening the impact of grading open channel Ca^{2+} flux, in essence, digitizing local Ca^{2+} signals arising from channel opening events. This led us to consider CaMKII as an on-the-spot integrator of L-type channel activity in E-T coupling. Direct experimental tests provided compelling evidence that CaMKII indeed acts as a local transducer of the frequency of L-type channel openings in rapid signaling to the nucleus.

Features of the signaling mechanism: bulk or local Ca^{2+}?

Functional analysis provided constraints on the molecular nature of L-type channel–pCREB coupling. We asked how, for a given total Ca^{2+} flux, signaling could be so much stronger with a high P_o and small i_{Ca} than with low P_o and large i_{Ca}. We tested various scenarios in which signal strength was dictated not simply by the size of the integrated Ca^{2+} influx but by channel gating. We found that the underlying mechanism must sense local Ca^{2+} transients near the channel, thus allowing brief and rapid fluctuations in local $[Ca^{2+}]$ to control signal strength. Three results weighed against bulk Ca^{2+} changes as the key determinant in signaling. First, involvement of bulk $[Ca^{2+}]$ increases generated by locally triggered RyRs were excluded because preventing RyR activity did not affect signal strength (Fig. S3). Second, similar bulk $[Ca^{2+}]$ elevations produced by either high P_o/small i_{Ca} or low P_o/large i_{Ca} produced very different outcomes. A bulk Ca^{2+} sensor distant from the channel could not provide such a distinction because of the blurring effects of Ca^{2+} diffusion from the channel's mouth. Third, we excluded the idea that bulk $[Ca^{2+}]$ is necessary for signaling, acting in concert with a readout of channel conformation. Conformational changes of L-type channels (without Ca^{2+} flux) had no effect on signaling when coupled with rises in bulk $[Ca^{2+}]$. These data indicate that, with the relatively mild depolarizations studied here, rises in bulk $[Ca^{2+}]$ are neither necessary nor sufficient for rapid signaling to CREB.

If not by raising bulk Ca^{2+}, how do L-type channels communicate with the nucleus? A remaining possibility is that the relevant Ca^{2+} signaling takes place in a domain near the point of entry (Chad and Eckert, 1984; Simon and Llinas, 1985; Augustine et al., 2003). At the inner mouth of the pore, $[Ca^{2+}]$ must increase in proportion to unitary flux to drive continual diffusion of Ca^{2+} away from the entry site (Klingauf and Neher, 1997). How could a sensor of this Ca^{2+} account for the steep dependence of signaling on P_o, but only mild dependence on i_{Ca}? In a
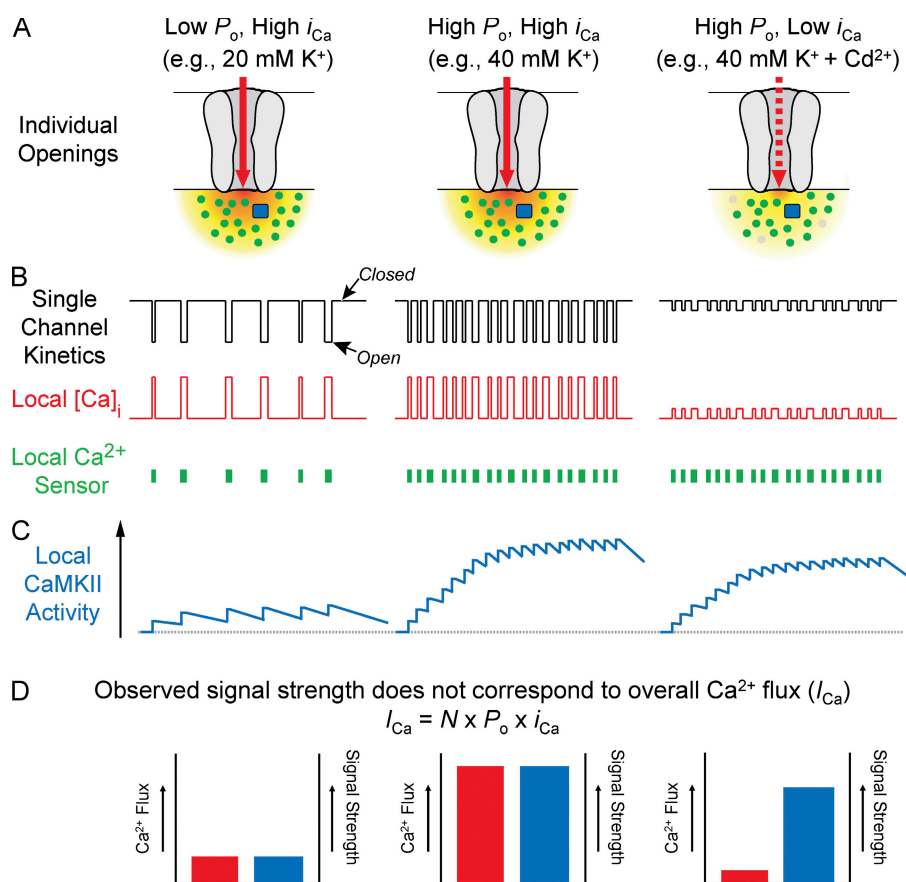
Figure 8. Model of local CaM saturation and frequency-dependent CaMKII activation. Schematic of the effects of three different types of stimulation on single channel kinetics and subsequent local effects on $[Ca^{2+}]$, Ca^{2+}/CaM levels, and CaMKII activity that lead to CREB phosphorylation in the nucleus. (A) Individual L-type channels in the open state. Ca^{2+} flows through the channel (red arrow) and results in a plume of Ca^{2+} near the pore (red/yellow gradient). Pore block with Cd^{2+} markedly decreases flux (dashed red arrow), resulting in a proportionately lower $[Ca^{2+}]$ in the plume. Local CaM molecules (dots) are either in the apo-CaM form (gray) or Ca^{2+} bound (green). A local CaM target (presumably CaMKII) is depicted as a blue square. (B) Schematized record of L-type channels opening briefly and intermittently during depolarization to give rise to unitary current (black). Closed intervals are abbreviated by increasing depolarization. Open channel current amplitude is decreased by Cd^{2+}. Local Ca^{2+} transients (red) mirror single channel currents, rising and falling quickly. During channel opening, the local Ca^{2+} levels saturate the local pool of apo-CaM, resulting in large elevations in Ca^{2+}/CaM even when Ca^{2+} transients are diminished by Cd^{2+}. Thus, transient elevations of Ca^{2+}/CaM, shown as solid green bars, match the channel openings in frequency but are not greatly affected by the magnitude of the single channel current. (C) Local Ca^{2+}/CaM pulses each have an incremental effect on local CaMKII activity (blue trace). With mild depolarization, pulses arrive at a low frequency and CaMKII activation decays between pulses. Upon stronger depolarization, interpulse intervals shorten and decay of activation is slowed by intersubunit phosphorylation, resulting in greater accumulation of CaMKII activation. This holds even when i_{Ca} is decreased with Cd^{2+}. (D) Schematic representation of data on CREB signal strength. The seemingly paradoxical finding that potent block of Ca^{2+} flux (red) with Cd^{2+} has a relatively weak effect on signal strength (blue) can be explained by local CaM saturation, allowing for potent local CaMKII activation even when Ca^{2+} flux is greatly decreased.

working model that emphasizes nanodomain signaling (Fig. 8 A), we propose that Ca^{2+} saturates a local sensor during each individual channel opening. As the membrane depolarizes and P_o increases, the channel's duty cycle shifts in favor of more openings, resulting in a steep increase in signal strength. In contrast, Cd^{2+} and La^{3+} sharply decreased i_{Ca} yet only mildly reduced signal strength. This is because the local Ca^{2+} rise due to a single open channel largely saturates the Ca^{2+} sensor so that decreasing flux has little effect on sensor activation. According to this scenario, local saturation transforms fluctuating Ca^{2+} signals into a digital format; depolarization encodes as the frequency of a series of binary pulses of Ca^{2+} sensor activity. The usefulness of digital encoding at the front end of a signaling pathway hinges on the existence of a decoder of pulse frequency, hence our consideration of CaMKII.

Recruitment of CaMKII as a steeply nonlinear reporter of channel activity

CaMKII has received little attention as a player in E-T coupling, but recent findings (Takeda et al., 2007) made it a plausible candidate. CaMKII tethers directly to L-type channels (Hudmon et al., 2005) and is thus well positioned to respond to Ca^{2+} sensors near the channel mouth. Furthermore, the multimeric structure of CaMKII supports intersubunit phosphorylation, and

thereby confers a steep dependence on the frequency of $Ca^{2+}/$ CaM pulses (De Koninck and Schulman, 1998; Dupont et al., 2003). Frequency-dependent activation of CaMKII is known to be important for Ca^{2+}-dependent facilitation of L-type channels themselves (Xiao et al., 1994; Yuan and Bers, 1994; Zuhlke et al., 1999; Hudmon et al., 2005).

Testing CaMKII led to four lines of evidence to support its participation in rapid signaling to the nucleus. First, the general CaMK inhibitor KN-93 blocked L-type channel-dependent signaling to pCREB. Second, upon L-type channel activation, pCaMKII puncta formed at the cell surface. Third, decreasing CaMKII levels reduced both the weight of pCaMKII puncta and the strength of CREB signaling. Fourth, pCaMKII formation was much more sensitive to changing P_o than i_{Ca}, thus accounting for the disparate effects on signaling to CREB. Collectively, these data provide compelling evidence that local CaMKII activation is critical in decoding Ca^{2+} transients generated by L-type channel openings. In line with local Ca^{2+} sensing, pCaMKII puncta appeared at or near the cell surface but did not translocate to the nucleus. This focuses attention on targets of CaMKII as likely participants in downstream signaling. CaM kinases are often able to act on each other as kinase kinases (Sugita et al., 1994; Soderling, 1999; Sakagami et al., 2005; Chow and Means, 2007), raising the possibility that CaMKII might lead to activation

Table I. **Features of excitation–response coupling**

	Coupling			
	E-S	Cardiac E-C	Skeletal E-C	E-T
Input–output speed	*ms*	*ms*	*ms*	*s–min*
Relationship to voltage (mV/e-fold change)	4.3[a]	6.2[b]	3.1[c]	**5.6**
Requires Ca^{2+} flux through membrane Ca^{2+} channels	Yes	Yes	No	Yes
Voltage dependence above and beyond Ca^{2+} flux	No	No	Yes	**Yes**
Locally mediated signaling	Yes	Yes	Yes	**Yes**
Requires Ca^{2+} release from stores	No	Yes	Yes	**No**
Target of Ca^{2+} or conformational coupling	synaptotagmin	RyRs	RyRs	**CaM/CaMKII**

Results in bold are from the present study.
[a]Katz and Miledi, 1967.
[b]Chapman and Tunstall, 1981.
[c]Hodgkin and Horowicz, 1960.

of a kinase like CaMKIδ, which along with CaM (Deisseroth et al., 1998; Sakagami et al., 2005) translocates to the nucleus upon depolarization (Sakagami et al., 2005).

The strong evidence for CaMKII raises the notion that CaM might be the saturating Ca^{2+} sensor proposed in our model (Fig. 8, green). What features of CaM would allow it to play such a role? We first considered that CaM binds the IQ motif within the C terminus of L-type channels (Zuhlke et al., 1999). IQ-bound CaM has been implicated in slow signaling to pCREB that relies on MAPK (Dolmetsch et al., 2001). However, the rapid signaling studied here is unlikely to involve this tethered CaM molecule. First, the IQ-bound CaM is tightly bound to the channel (Erickson et al., 2001; Pitt et al., 2001) and cannot simultaneously bind the channel and activate target enzymes. Second, a single tethered CaM would be insufficient to trigger persistent activation of CaMKII, which has ≥12 Ca^{2+}/CaM binding sites and requires binding of multiple CaMs to drive autophosphorylation (Hanson and Schulman, 1992). More likely, CaMKII is activated by the large pool of ∼25 mobile apo-CaM molecules that reside within 40 nm of the channel mouth (Mori et al., 2004). The millimolar peak levels of $[Ca^{2+}]_i$ attained when channels are open will far exceed CaM's EC_{50} of 5–10 μM (Burgoyne, 2007), thereby saturating the local cadre of apo-CaM.

With mild depolarization, the frequency of L-type channel openings would be low enough to allow Ca^{2+} to dissociate from CaM and/or for Ca^{2+}/CaM to diffuse away from its target between openings. Thus, pulsatile Ca^{2+} entry will be converted to brief, pulse-like surges of Ca^{2+}/CaM, with the same temporal pattern as the channel openings (Fig. 8 B, middle). Even when Ca^{2+} influx is sharply reduced (e.g., by Cd^{2+} block), the local Ca^{2+} rise would still be sufficient to activate most of the local CaM molecules (Fig. 8 A, right), hence the shallow dependence on the open channel Ca^{2+} flux (Fig. 8 B, right). In contrast, varying the level of depolarization would sharply alter the frequency of channel openings, in turn strongly affecting the pattern of local Ca^{2+}/CaM rises and thus the extent to which CaMKII is activated and autophosphorylated, which is in line with its well described frequency dependence (De Koninck and Schulman, 1998; Dupont et al., 2003). With mild depolarization, unitary openings and Ca^{2+}/CaM pulses are infrequent, CaM largely dissociates from CaMKII during the interpulse interval, and CaMKII activity is low. With

stronger depolarization, unitary openings come in rapid succession, leaving less time for CaM dissociation, resulting in greater temporal summation and more CaMKII activation. When adjacent subunits bind Ca^{2+}/CaM, they reciprocally prolong their activated state through autophosphorylation and CaM trapping, a steeply frequency-dependent process. Further, because decreasing Ca^{2+} flux through open channels has little effect on Ca^{2+}/CaM elevations, local CaMKII activation is largely dictated by the frequency of channel openings and not the magnitude of the open channel Ca^{2+} flux, thus accounting for the dichotomous dependences of pCaMKII on P_o and i_{Ca} (Fig. 5 D). Finding that pCaMKII is less steeply voltage dependent than pCREB may indicate that CREB signaling is mediated by the cooperative action of multiple L-type channel–CaMKII complexes.

A remaining issue is whether there is any role for a voltage-dependent conformational change. We ruled out a critical role of conformational changes working in conjunction with bulk Ca^{2+}, but did not exclude a conformational change working in coordination with local Ca^{2+} signaling. The latter scenario gains credence from experiments where immobilizing the Ca^{2+} channel's C terminus prevented CREB phosphorylation but spared Ca^{2+} influx (Kobrinsky et al., 2003). A depolarization-driven conformational change in the L-type channel could support kinase activation or allow the activated kinase to access its target (Artalejo et al., 1992). Such possibilities have already been proposed for voltage-dependent facilitation (Hoshi et al., 1984; Pietrobon and Hess, 1990; Artalejo et al., 1992), another CaMKII-dependent process (Xiao et al., 1994; Lee et al., 2006).

Further structural information on the L-type channel–CaMKII interaction will help clarify whether a direct interaction is necessary for signaling to CREB. CaMKII interactions with the $Ca_V1.2$ (α_{1C}) L-type channel are supported by binding determinants within multiple cytoplasmic loops; SCG neurons express multiple CaMKII isoforms and multiple L-type isoforms ($Ca_V1.2$ and $Ca_V1.3$). A first step will be to determine whether structural determinants of αCaMKII binding to $Ca_V1.2$ (Hudmon et al., 2005) generalize to other kinase and channel isoforms.

Comparisons with E-C and E-S coupling

The steep voltage dependence of E-T coupling was comparable to that found in classical studies of E-C and E-S coupling

(Hodgkin and Horowicz, 1960; Katz and Miledi, 1967; Chapman and Tunstall, 1981; Table I). In the case of contraction, skeletal E-C coupling is independent of Ca^{2+} flux (Armstrong et al., 1972), whereas E-T coupling requires at least minimal Ca^{2+} influx (Greenberg et al., 1986; Morgan and Curran, 1986; Fig. 1 A), indicating divergent mechanisms. E-T coupling is more comparable to cardiac E-C coupling, wherein Ca^{2+} flux through L-type channels is necessary to activate RyR (Bers, 2002), and RyR activity is proportional to the square of the local $[Ca^{2+}]$ (Santana et al., 1996). Interestingly, the "gain" of L-type channel coupling to RyRs decreases at stronger depolarizations, possibly reflecting some kind of saturation (Altamirano and Bers, 2007), akin to what we infer here. However, in cardiac E-C coupling, RyRs are absolutely required, and gradations in i_{Ca} or P_o have largely similar effects on RyR function (Altamirano and Bers, 2007). Thus, E-T coupling is mechanistically different from both cardiac and skeletal E-C coupling.

Our finding that CREB signal strength follows $[Ca^{2+} flux]^{2-3}$ is reminiscent of E-S coupling, where the corresponding exponent is 3–5 (Dodge and Rahamimoff, 1967; Augustine et al., 1985; Bollmann et al., 2000; Schneggenburger and Neher, 2000; for review see Augustine, 2001). Importantly, the steep Ca^{2+} dependence of secretion, caused by multiple Ca^{2+} ions acting on synaptotagmin Ca^{2+} sensors (Sudhof, 2004), is maintained even when i_{Ca} is graded (Wu and Saggau, 1994; Mintz et al., 1995; Shahrezaei et al., 2006). In this respect, E-S coupling contrasts sharply with E-T coupling, in which grading Ca^{2+} flux with Cd^{2+} reveals a distinct, shallow relationship.

L-type channel signaling from a broader functional perspective

We focused on steady depolarization over a relatively negative voltage range as a way of defining the limiting voltage dependence of E-T coupling (Almers, 1978). Under these conditions L-type channels dominate signaling, an advantage for mechanistic studies. For this purpose, using action potentials would be interesting, but also complicated, as they sweep rapidly through a wide range of voltages and drive activation of multiple Ca^{2+} channel types. In fact, Ca_V2 channels recruited by strong depolarization also signal to CREB (Wheeler, D.G., C.F. Barrett, and R.W. Tsien. 2007. Society for Neuroscience Annual Meeting. Abstr. 784.20), accounting for the ability of non–L-type channels to contribute to signaling to CREB with repetitive spiking (Brosenitsch and Katz, 2001; Zhao et al., 2007). Interestingly, signaling by Ca_V2 channels is dependent on bulk $[Ca^{2+}]$ (compare with Hardingham et al., 2001), in striking contrast to the L-type channel–dedicated, local Ca^{2+}/CaMKII-dependent mechanism described here. The importance of L-type Ca^{2+} channels may be further enhanced by an atypical gating in which, after a delay, some of the channels open upon repolarization after a previous strong depolarization (Pietrobon and Hess, 1990; Kavalali and Plummer, 1994; Koschak et al., 2007). Such gating would not be triggered by the stimuli we used, but might become significant with repetitive action potentials as stimuli.

Our results have functional implications for CRE-dependent gene expression, which requires long lasting CREB phosphorylation (Bito et al., 1996). Under physiological conditions, neurons undergo bouts of depolarizing activity (e.g., bursts of spikes, synaptic depolarizations, upstates, and/or tonic depolarization triggered by G protein–coupled receptors). Although individual units of physiological activity may be too brief to induce gene expression, a series of such bouts, each with an incremental effect on pCREB, will enhance and prolong CREB phosphorylation, thus engaging transcription. Thus, our findings on the voltage and time dependence of CREB phosphorylation shed light on the dynamics of signaling by single bouts of depolarization and give insight into the underlying mechanisms.

Materials and methods

Cell culture
SCG neurons were dissected from postnatal day 0–1 Sprague-Dawley rats and incubated for 30 min at 37°C in a solution containing 15 mg/ml trypsin (Sigma-Aldrich). Cells were then washed, dissociated by trituration with a fire-polished, siliconized Pasteur pipette, and plated on laminin/poly-L-lysine–coated glass coverslips (BD) in 24-well plates. The cultures were maintained in 5% CO_2 at 37°C in L-15 medium (Invitrogen) supplemented with sodium bicarbonate, penicillin/streptomycin, glucose, 10% FBS, 25 ng/ml of nerve growth factor, and a vitamin mix (Hawrot and Patterson, 1979). Cultures were fed 1 d after plating by replacing half the medium with medium containing 5 µM of cytosine arabinoside and were subsequently fed every third day. In all experiments, neurons were used 4–6 d after plating.

Adenovirus production and infection
SCG neurons were infected with an adenovirus expressing a dihydropyridine-insensitive L-type ($\alpha_{1C,77}$) channel driven by the synapsin I promoter as previously described (Wheeler and Cooper, 2001; Wheeler et al., 2006). Near 100% infection efficiency was achieved by adding ∼50 infectious particles per microliter to the growth medium (1.5 ml in 1 well of a 24-well plate) 1 d after plating.

Stimulation and immunocytochemistry
We induced CREB phosphorylation in two different ways. To measure isochronic pCREB levels (Fig. 1, A and B), cells were stimulated at room temperature with the indicated high $[K^+]$ solution for 3 min, and then immediately fixed. To measure signal strength we used a ballistic protocol wherein cells were stimulated with high $[K^+]$ for the indicated time and then placed in control (5 mM K^+) solution for a given period of time before fixation. In Fig. 1 (C–F), the stimulation time plus the delay before fixation totaled 3 min, allowing direct comparison with the data in Fig. 1 (A and B). A series of control experiments with various $[K^+]$ and stimulus durations revealed that a 45-s delay in control solution provides maximal phosphorylation of CREB; beyond this time, pCREB levels decline, reaching baseline levels within a few minutes. Therefore, in all experiments measuring CREB signal strength, except those in Fig. 1, the delay between stimulation and fixation was set at 45 s (see Fig. S1).

Control solution (5-mM K^+ Tyrode's) consisted of 150 mM NaCl, 5 mM KCl, 2 mM $MgCl_2$, 2 mM $CaCl_2$, 10 mM Hepes, and 10 mM glucose, pH 7.3. When stimulating with elevated $[K^+]$, Na^+ was reduced to maintain osmolarity. The Ca^{2+}-free solution was prepared by replacing the $CaCl_2$ with $MgCl_2$ and adding 0.5 mM EGTA. Before stimulation, cells were pretreated with 0.5 µM tetrodotoxin (TTX), which remained present during stimulation. In experiments with Cd^{2+} or La^{3+}, the ions were applied only at the time of stimulation or 1 s before.

Cells were fixed in ice-cold 4% paraformaldehyde in phosphate buffer supplemented with 4% (wt/vol) sucrose. Fixed cells were then permeabilized with Triton X-100, blocked with 6% normal goat serum, and incubated overnight at 4°C in primary antibodies: rabbit anti-pCREB (1:133 dilution; Cell Signaling Technology); mouse anti-MAP2 antibody (HM-2; 1:1,000; Sigma-Aldrich); rabbit anti-pCaMKII against Thr286 of αCaMKII or Thr287 of βCaMKII (1:10,000; Cell Signaling Technology); mouse anti-βCaMKII (1:200; Invitrogen). The next day, neurons were washed with PBS, incubated at room temperature for 45 min in a 1:200 dilution of anti-rabbit–Alexa488 and/or anti-mouse–Alexa568 (Invitrogen), washed with PBS, and mounted using VECTASHIELD mounting medium with DAPI (Vector Laboratories). The cells were imaged through a 40× (1.3 NA) oil objective on an epifluorescent microscope (Axioplan) equipped with a digital camera (AxioCam) using AxioVision 3.1 (all from Carl Zeiss, Inc.).

Electrophysiology

Whole-cell voltage- and current-clamp recordings were performed at room temperature (20–22°C) using a patch-clamp amplifier (Axopatch 200B; MDS Analytical Technology). Patch pipettes were pulled in a puller (P-97; Sutter Instrument Co.) from borosilicate glass capillaries and heat polished before use with a microforge (MF-9; Narishige). Pipette resistance was ∼2–4 MΩ when filled with internal solution. For current-clamp recordings, the bath solution was the same Tyrode's solution used for CREB phosphorylation experiments, containing 2 mM Ca^{2+}, and the pipette contained 122 mM of potassium gluconate, 9 mM NaCl, 1.8 mM $MgCl_2$, 0.9 mM EGTA, 5 mM ATP, 0.5 mM GTP, 9 mM Hepes, and 14 mM phosphocreatine, pH 7.3; for some recordings, 0.5 µM TTX was included in the bath solution to block action potentials. For recording whole-cell Ca^{2+} currents in voltage clamp, again the bath solution was the same 2-mM Ca^{2+} Tyrode's solution used in pCREB experiments, supplemented with 1 mM TEA and 0.5 µM TTX, and the pipette contained 122 mM Cs-Asp, 10 mM Hepes, 10 mM EGTA, 5 mM $MgCl_2$, 4 mM ATP, and 0.4 mM GTP, pH 7.5. The traces shown are the mean of 10 consecutive sweeps.

Bath solution exchanges were performed via gravity-fed perfusion, with complete volume exchange in <5 s. Series resistance was compensated electronically by ≥90%, and membrane capacitance was corrected online; residual linear capacitive and leak currents were subtracted by the −$P/4$ method. Data were passed through a 4-pole low-pass Bessel filter, digitized using a Digidata 1320A (MDS Analytical Technology), and stored on a personal computer for offline analysis. Currents were filtered at 1–2 kHz and digitized at 2–20 kHz. Pulse depolarizations were applied at 10-s intervals.

Ca^{2+} imaging

SCG neurons were loaded for 30–60 min with 2 µM Fura-2 AM (Invitrogen) and 0.02% Pluronic F-127 (Invitrogen) in conditioned SCG growth medium in a 37°C/5% CO_2 incubator. Fura-2 fluorescence, measured at 0.33 Hz, was elicited by excitation at 340 and 380 nm, detected at 510 nm, and imaged with a charge coupled device camera (C4742-95 Orca; Hamamatsu Photonics). The 340/380 ratio was quantified using regions of interest outlining the entire cell body. After background subtraction, ratios were converted to $[Ca^{2+}]_i$ based on an empirical fit of ratios obtained from a Fura-2 Ca^{2+} imaging calibration kit (Invitrogen). Bath solution exchanges were performed via gravity-fed perfusion, with 50% volume exchange in <2 s. When measuring the effect of grading single channel current, Cd^{2+} was applied 30 s before the K^+ challenge. In experiments with La^{3+}, there was no La^{3+} preincubation. The solutions used were the same as described above for pCREB stimulation, and all solutions contained 0.5 µM TTX.

Lentiviral-mediated knockdown of αCaMKII and βCaMKII

The self-inactivating bicistronic lentiviral transfer vector construct pLVTHM and the second generation lentivirus packaging and envelope plasmids were provided by D. Trono (University of Geneva, Geneva, Switzerland) (Wiznerowicz and Trono, 2003).The pLVTHM lentiviral vector carries the EF1α promoter to drive GFP and the H1 RNA polymerase III promoter to permit the expression of an shRNA for RNA interference (Wiznerowicz and Trono, 2003). Two complementary DNA oligonucleotides (Operon Biotechnologies, Inc.) were annealed to produce a double-stranded DNA fragment encoding a 19-nucleotide sense strand (uppercase), 9-nucleotide loop (lowercase italicized), and 19-nucleotide antisense strand (uppercase) of the αCaMKII, βCaMKII, or nonsilencing sequence. The sequence of the αCaMKII shRNA is as follows: 5′-cgcgtccccGAATGATGGCGTG-AAGGAA*ttcaagaga*TTCCTTCACGCCATCATTCtttttggaaat-3′ (sense) and 5′-cgatttccaaaaaGAATGATGGCGTGAAGGAA*tctcttgaa*TTCCTTCACG-CCATCATTCgggga-3′ (antisense). The αCaMKII target sequence corresponds to bases 1010–1028 of the αCaMKII mRNA (GenBank/EMBL/DDBJ accession no. NM_012920). The βCaMKII shRNA (5′-cgcgtccccGAGTAT-GCAGCTAAGATCA*ttcaagaga*TGATCTTAGCTGCATACTCtttttggaaat-3′ [sense] and 5′-cgatttccaaaaaGAGTATGCAGCTAAGATCA*tctcttgaa*TGA-TCTTAGCTGCATACTCggggga [antisense]) targets bases 197–215 of the βCaMKII mRNA (GenBank/EMBL/DDBJ accession no. NM_021739). We also used an shRNA with a nonsilencing target sequence: 5′-cgcgt-ccccTCGCTTGGGCGAGAGTAAG*ttcaagaga*CTTACTCTCGCCCAAGC-GAtttttggaaat-3′ (sense) and 5′-cgatttccaaaaaTCGCTTGGGCGAGAGTA-AG*tctcttgaa*CTTACTCTCGCCCAAGCGAggggga-3′ (antisense).

The duplex DNAs of shRNA-αCaMKII, shRNA-βCaMKII, and shRNA-nonsilencing were cloned into the MluI and ClaI sites of the pLVTHM vector. After confirming the ability of each shRNA to knock down their intended targets in HEK293T cells overexpressing wild-type αCaMKII or βCaMKII,

viral particles were produced by transfection (Lipofectamine 2000; Invitrogen) of 293T cells plated in 100-mm dishes in DME plus 10% FBS. Subconfluent 293T cells were cotransfected with 10 µg of lentiviral vector containing the transgene, 7.5 µg of the packaging plasmid psPAX2, and 3 µg of the envelope plasmid pMD2.g. After 16 h, the medium was changed. The supernatant was collected 24 h later (∼10 ml per dish) and cleared of cell debris by filtering through a 0.45-µm filter. The viral particles were concentrated by ultracentrifugation of the filtrate at 70,000 g for 2 h at 4°C using a rotor (SW28; Beckman Coulter). The viral pellet was then resuspended in sterile PBS, aliquoted, and stored at −80°C. Lentivirus particles (0.15–0.5 µl of viral stock diluted in 20 µl PBS per coverslip) were added to SCG cultures containing 500 µl of medium the day after plating. 24 h later, the cultures were fed with 1 ml of medium and used 3 d later, when GFP could be detected in ∼100% of the neurons.

Real-time PCR

4 d after infection, the medium was replaced with the RNA stabilization reagent RNA*Later* (QIAGEN) and the cells were stored at 4°C until use. Total RNA was isolated from cultured cells using the RNeasy Micro kit (QIAGEN) and reverse transcribed into cDNA using a QuantiTect RT-PCR kit (QIAGEN), as per the manufacturer's instructions. Each sample was from one 12-mm coverslip containing ∼50–100 neurons. Real-time PCR studies were performed with DyNAmo HS SYBR Green Master Mix (Finnzymes) using the DNA engine Opticon 2 (Bio-Rad Laboratories) through 45 PCR cycles (94°C for 10 s, 60°C for 30 s, and 72°C for 30 s). In each experiment, three separate coverslips were used per condition and each cDNA sample, equivalent to RNA from one well of cultured cells (24-well plate), was run in duplicate for the target genes (αCaMKII and βCaMKII) and the housekeeping genes (β-actin, α-tubulin, and GAPDH). Specificity of amplicons was determined by melting curve analysis, gel electrophoresis, and DNA sequencing. Primer pair sequences were as follows: αCaMKII (GenBank/EMBL/DDBJ accession no. NM_012920), forward primer 5′-CTCTGAGAGCACCAACACCA-3′ (nucleotides 1031–1050) and reverse primer 5′-CCATTGCTTATGGCTTCGAT-3′ (1113–1132); βCaMKII (M16112), forward primer 5′-GTCCACCGCGGCCTC-3′ (1040–1054) and reverse primer 5′-TTTTGGTGCTGTTTGTCTGGG-3′ (1123–1143); β-actin (NM_03144), forward primer 5′-AGGCCCCTCTGAACCCTAAG-3′ (401–420) and reverse primer 5′-CCAGAGGCATACAGGGACAAC-3′ (498–519); α-tubulin (GenBank/EMBL/DDBJ accession no. NM_001007004), forward primer 5′-GAGATCCGAAATGGCCCGTAC-3′ (263–283) and reverse primer 5′-GCCAATGGTGTAGTGACCACG-3′ (347–367); GAPDH (GenBank/EMBL/DDBJ accession no. NM_017008), forward primer 5′-AACCTGCCAAGTATGATGACATCA-3′(822–845) and reverse primer 5′-TGTTGAAGTCACAGGAGCAACCT-3′ (909–932). All primers were synthesized by Operon Biotechnologies, Inc.

The relative mRNA levels were calculated by normalization of cycle threshold (C(t)) values of the target gene (αCaMKII and βCaMKII) to each of the reference genes (β-actin, α-tubulin, and GAPDH) using the comparative C(t) ($\Delta\Delta C(t)$) method, where $\Delta C(t)$ values were calculated from the following three equations: (1) $\Delta C(t)$treatment = C(t)target − C(t)reference; (2) $\Delta C(t)$control = C(t)target − C(t)reference; and (3) $\Delta\Delta C(t) = \Delta C(t)$treatment − $\Delta C(t)$control.

Data are reported as the mean ratio of fold change in the mRNA of interest corrected for each reference gene ($2^{-\Delta\Delta C(t)}$). The control group was always the empty vector condition, thus the ratio of 1. Real-time PCR experiments were analyzed using one-way analysis of variance with Student-Newman-Keuls Multiple Comparisons post hoc (p-values) tests. Differences between means were considered a priori as significant at $P < 0.05$.

Data analysis

Electrophysiology data were acquired and analyzed using Clampex 8.2 and Clampfit 8.2, respectively (MDS Analytical Technologies). The exponential fits in Fig. 2 E were calculated using the equation $y = y_0 + A \times e^{(x/k)}$, where y is Ca^{2+} flux or pCREB signal strength, y_0 is the pedestal, A is amplitude, and k is given in mV/e-fold change in y. Unless otherwise indicated, in electrophysiology and Fura-2 imaging experiments, sample size represents the number of individual cells recorded or analyzed. Data are presented as mean ± SEM. When not stated, p-values are from Students' t tests.

Image analysis

We quantified pCREB staining using Axiovision LE 4.2 (Carl Zeiss, Inc.). The nuclear marker, DAPI, and an antibody against the neuron-specific protein MAP2 were used to delineate neuronal nuclei, which were used as regions of interest. Mean pixel intensity in the pCREB channel was measured using these regions of interest and the "off-cell" background

measured near the cell was subtracted. To determine CREB signal strength, in individual experiments the mean pCREB level in control (unstimulated) cells was considered as baseline and set to 0% and the pCREB level after a 3-min, 40-mM K+ stimulation was set to maximum (i.e., 100%). The slope of the initial relationship between stimulation time and pCREB level in a given experiment was used as a measure of CREB signal strength, units being percentage per second. Where indicated, signal strength under each condition was normalized to the strength in 40 mM K+ to correct for slight culture-to-culture variations.

To measure pCaMKII puncta, we captured 8-bit epifluorescent images and subtracted background staining using the rolling ball method (Sternberg, 1983) in ImageJ (National Institutes of Health; for theoretical analysis of a similar approach, see Mager et al., 2007). After subtraction, we thresholded images such that only those pixels 5 units (0–255 scale) above background remained. We then classified puncta as regions with a minimum of four adjacent suprathreshold pixels. For each punctum, the product of the punctum size and mean pixel intensity (above background) was used as a read-out of the magnitude of the local pCaMKII response or the punctum weight. The sum of all puncta on an individual cell gave its pCaMKII puncta weight.

Online supplemental material
Fig. S1 shows that two protocols for measuring CREB signal strength differ strongly in absolute terms but yield similar estimates of the steep dependence on [K+]o and hence membrane potential. Fig. S2 shows that CREB signal strength is steeply dependent on L-type channel activity. Fig. S3 shows that RyRs do not account for the importance of P_o in determining CREB signal strength. Fig. S4 shows that La^{3+}-mediated inhibition of single channel flux potently blocks rises in [Ca^{2+}]$_i$ but has very little effect on CREB signal strength. Online supplemental material is available at http://www.jcb.org/cgi/content/full/jcb.200805048/DC1.

References

Adams, P.R., and D.A. Brown. 1973. Action of -aminobutyric acid (GABA) on rat sympathetic ganglion cells. *Br. J. Pharmacol.* 47:639P–640P.

Almers, W. 1978. Gating currents and charge movements in excitable membranes. *Rev. Physiol. Biochem. Pharmacol.* 82:96–190.

Altamirano, J., and D.M. Bers. 2007. Voltage dependence of cardiac excitation-contraction coupling: unitary Ca2+ current amplitude and open channel probability. *Circ. Res.* 101:590–597.

Armstrong, C.M., F.M. Bezanilla, and P. Horowicz. 1972. Twitches in the presence of ethylene glycol bis(-aminoethyl ether)-N,N'-tetracetic acid. *Biochim. Biophys. Acta.* 267:605–608.

Artalejo, C.R., S. Rossie, R.L. Perlman, and A.P. Fox. 1992. Voltage-dependent phosphorylation may recruit Ca2+ current facilitation in chromaffin cells. *Nature.* 358:63–66.

Augustine, G.J. 2001. How does calcium trigger neurotransmitter release? *Curr. Opin. Neurobiol.* 11:320–326.

Augustine, G.J., M.P. Charlton, and S.J. Smith. 1985. Calcium entry and transmitter release at voltage-clamped nerve terminals of squid. *J. Physiol.* 367:163–181.

Augustine, G.J., F. Santamaria, and K. Tanaka. 2003. Local calcium signaling in neurons. *Neuron.* 40:331–346.

Beam, K.G., and C. Franzini-Armstrong. 1997. Functional and structural approaches to the study of excitation-contraction coupling. *Methods Cell Biol.* 52:283–306.

Berridge, M.J. 1998. Neuronal calcium signaling. *Neuron.* 21:13–26.

Bers, D.M. 2002. Cardiac excitation-contraction coupling. *Nature.* 415:198–205.

Bers, D.M., and T. Guo. 2005. Calcium signaling in cardiac ventricular myocytes. *Ann. NY Acad. Sci.* 1047:86–98.

Bito, H., K. Deisseroth, and R.W. Tsien. 1996. CREB phosphorylation and dephosphorylation: a Ca(2+)- and stimulus duration-dependent switch for hippocampal gene expression. *Cell.* 87:1203–1214.

Bollmann, J.H., B. Sakmann, and J.G. Borst. 2000. Calcium sensitivity of glutamate release in a calyx-type terminal. *Science.* 289:953–957.

Brosenitsch, T.A., and D.M. Katz. 2001. Physiological patterns of electrical stimulation can induce neuronal gene expression by activating N-type calcium channels. *J. Neurosci.* 21:2571–2579.

Burgoyne, R.D. 2007. Neuronal calcium sensor proteins: generating diversity in neuronal Ca2+ signalling. *Nat. Rev. Neurosci.* 8:182–193.

Cannell, M.B., H. Cheng, and W.J. Lederer. 1995. The control of calcium release in heart muscle. *Science.* 268:1045–1049.

Carlezon, W.A. Jr., R.S. Duman, and E.J. Nestler. 2005. The many faces of CREB. *Trends Neurosci.* 28:436–445.

Chad, J.E., and R. Eckert. 1984. Calcium domains associated with individual channels can account for anomalous voltage relations of CA-dependent responses. *Biophys. J.* 45:993–999.

Chapman, R.A., and J. Tunstall. 1981. The tension-depolarization relationship of frog atrial trabeculae as determined by potassium contractures. *J. Physiol.* 310:97–115.

Chow, F., and A. Means. 2007. The calcium/calmodulin-dependent protein kinase cascades. *In* Calcium: A Matter of Life or death. Vol. 41. J. Krebs and M. Michalak, editors. Elsevier B.V., Amsterdam. 345–364.

Chow, R.H. 1991. Cadmium block of squid calcium currents. Macroscopic data and a kinetic model. *J. Gen. Physiol.* 98:751–770.

De Crescenzo, V., K.E. Fogarty, R. Zhuge, R.A. Tuft, L.M. Lifshitz, J. Carmichael, K.D. Bellve, S.P. Baker, S. Zissimopoulos, F.A. Lai, et al. 2006. Dihydropyridine receptors and type 1 ryanodine receptors constitute the molecular machinery for voltage-induced Ca2+ release in nerve terminals. *J. Neurosci.* 26:7565–7574.

De Koninck, P., and H. Schulman. 1998. Sensitivity of CaM kinase II to the frequency of Ca2+ oscillations. *Science.* 279:227–230.

Deisseroth, K., H. Bito, and R.W. Tsien. 1996. Signaling from synapse to nucleus: postsynaptic CREB phosphorylation during multiple forms of hippocampal synaptic plasticity. *Neuron.* 16:89–101.

Deisseroth, K., E.K. Heist, and R.W. Tsien. 1998. Translocation of calmodulin to the nucleus supports CREB phosphorylation in hippocampal neurons. *Nature.* 392:198–202.

Deisseroth, K., P.G. Mermelstein, H. Xia, and R.W. Tsien. 2003. Signaling from synapse to nucleus: the logic behind the mechanisms. *Curr. Opin. Neurobiol.* 13:354–365.

Dodge, F.A. Jr., and R. Rahamimoff. 1967. Co-operative action a calcium ions in transmitter release at the neuromuscular junction. *J. Physiol.* 193:419–432.

Dolmetsch, R. 2003. Excitation-transcription coupling: signaling by ion channels to the nucleus. *Sci. STKE.* 2003:PE4.

Dolmetsch, R.E., U. Pajvani, K. Fife, J.M. Spotts, and M.E. Greenberg. 2001. Signaling to the nucleus by an L-type calcium channel-calmodulin complex through the MAP kinase pathway. *Science.* 294:333–339.

Dupont, G., G. Houart, and P. De Koninck. 2003. Sensitivity of CaM kinase II to the frequency of Ca2+ oscillations: a simple model. *Cell Calcium.* 34:485–497.

Ellinor, P.T., J. Yang, W.A. Sather, J.F. Zhang, and R.W. Tsien. 1995. Ca2+ channel selectivity at a single locus for high-affinity Ca2+ interactions. *Neuron.* 15:1121–1132.

Erickson, M.G., B.A. Alseikhan, B.Z. Peterson, and D.T. Yue. 2001. Preassociation of calmodulin with voltage-gated Ca(2+) channels revealed by FRET in single living cells. *Neuron.* 31:973–985.

Franzini-Armstrong, C., and F. Protasi. 1997. Ryanodine receptors of striated muscles: a complex channel capable of multiple interactions. *Physiol. Rev.* 77:699–729.

Greenberg, M.E., E.B. Ziff, and L.A. Greene. 1986. Stimulation of neuronal acetylcholine receptors induces rapid gene transcription. *Science.* 234:80–83.

Guatimosim, S., K. Dilly, L.F. Santana, M. Saleet Jafri, E.A. Sobie, and W.J. Lederer. 2002. Local Ca(2+) signaling and EC coupling in heart: Ca(2+) sparks and the regulation of the [Ca(2+)](i) transient. *J. Mol. Cell. Cardiol.* 34:941–950.

Hagiwara, S., and K. Takahashi. 1967. Surface density of calcium ions and calcium spikes in the barnacle muscle fiber membrane. *J. Gen. Physiol.* 50:583–601.

Hanson, P.I., and H. Schulman. 1992. Neuronal Ca2+/calmodulin-dependent protein kinases. *Annu. Rev. Biochem.* 61:559–601.

Hardingham, G.E., F.J. Arnold, and H. Bading. 2001. Nuclear calcium signaling controls CREB-mediated gene expression triggered by synaptic activity. *Nat. Neurosci.* 4:261–267.

Hawrot, E., and P.H. Patterson. 1979. Long-term culture of dissociated sympathetic neurons. *Methods Enzymol.* 58:574–584.

Hegle, A.P., D.D. Marble, and G.F. Wilson. 2006. A voltage-driven switch for ion-independent signaling by ether-a-go-go K+ channels. *Proc. Natl. Acad. Sci. USA.* 103:2886–2891.

Henkart, M. 1980. Identification and function of intracellular calcium stores in axons and cell bodies of neurons. *Fed. Proc.* 39:2783–2789.

Hille, B. 1994. Modulation of ion-channel function by G-protein-coupled receptors. *Trends Neurosci.* 17:531–536.

Hille, B. 2001. Ion Channels of Excitable Membranes. Sinauer, Sunderland, MA. 814 pp.

Hirning, L.D., A.P. Fox, E.W. McCleskey, B.M. Olivera, S.A. Thayer, R.J. Miller, and R.W. Tsien. 1988. Dominant role of N-type Ca2+ channels in evoked release of norepinephrine from sympathetic neurons. *Science.* 239:57–61.

Hodgkin, A.L., and P. Horowicz. 1960. Potassium contractures in single muscle fibres. *J. Physiol.* 153:386–403.

Hoshi, T., J. Rothlein, and S.J. Smith. 1984. Facilitation of Ca2+-channel currents in bovine adrenal chromaffin cells. *Proc. Natl. Acad. Sci. USA.* 81:5871–5875.

Hudmon, A., H. Schulman, J. Kim, J.M. Maltez, R.W. Tsien, and G.S. Pitt. 2005. CaMKII tethers to L-type Ca^{2+} channels, establishing a local and dedicated integrator of Ca^{2+} signals for facilitation. *J. Cell Biol.* 171:537–547.

Kaczmarek, L.K. 2006. Non-conducting functions of voltage-gated ion channels. *Nat. Rev. Neurosci.* 7:761–771.

Katz, B., and R. Miledi. 1967. A study of synaptic transmission in the absence of nerve impulses. *J. Physiol.* 192:407–436.

Kavalali, E.T., and M.R. Plummer. 1994. Selective potentiation of a novel calcium channel in rat hippocampal neurones. *J. Physiol.* 480:475–484.

Klingauf, J., and E. Neher. 1997. Modeling buffered Ca2+ diffusion near the membrane: implications for secretion in neuroendocrine cells. *Biophys. J.* 72:674–690.

Kobrinsky, E., E. Schwartz, D.R. Abernethy, and N.M. Soldatov. 2003. Voltage-gated mobility of the Ca2+ channel cytoplasmic tails and its regulatory role. *J. Biol. Chem.* 278:5021–5028.

Koschak, A., G.J. Obermair, F. Pivotto, M.J. Sinnegger-Brauns, J. Striessnig, and D. Pietrobon. 2007. Molecular nature of anomalous L-type calcium channels in mouse cerebellar granule cells. *J. Neurosci.* 27:3855–3863.

Kunze, D.L., and D. Rampe. 1992. Characterization of the effects of a new Ca2+ channel activator, FPL 64176, in GH3 cells. *Mol. Pharmacol.* 42:666–670.

Lansman, J.B., P. Hess, and R.W. Tsien. 1986. Blockade of current through single calcium channels by Cd^{2+}, Mg^{2+}, and Ca^{2+}. Voltage and concentration dependence of calcium entry into the pore. *J. Gen. Physiol.* 88:321–347.

Lee, T.S., R. Karl, S. Moosmang, P. Lenhardt, N. Klugbauer, F. Hofmann, T. Kleppisch, and A. Welling. 2006. Calmodulin kinase II is involved in voltage-dependent facilitation of the L-type Cav1.2 calcium channel: identification of the phosphorylation sites. *J. Biol. Chem.* 281:25560–25567.

Lencesova, L., A. O'Neill, W.G. Resneck, R.J. Bloch, and M.P. Blaustein. 2004. Plasma membrane-cytoskeleton-endoplasmic reticulum complexes in neurons and astrocytes. *J. Biol. Chem.* 279:2885–2893.

Lin, Z., C. Harris, and D. Lipscombe. 1996. The molecular identity of Ca channel alpha 1-subunits expressed in rat sympathetic neurons. *J. Mol. Neurosci.* 7:257–267.

Liu, L., P.K. Gonzalez, C.F. Barrett, and A.R. Rittenhouse. 2003. The calcium channel ligand FPL 64176 enhances L-type but inhibits N-type neuronal calcium currents. *Neuropharmacology.* 45:281–292.

Llinas, R., I.Z. Steinberg, and K. Walton. 1981. Relationship between presynaptic calcium current and postsynaptic potential in squid giant synapse. *Biophys. J.* 33:323–351.

Lonze, B.E., and D.D. Ginty. 2002. Function and regulation of CREB family transcription factors in the nervous system. *Neuron.* 35:605–623.

Lopez-Lopez, J.R., P.S. Shacklock, C.W. Balke, and W.G. Wier. 1995. Local calcium transients triggered by single L-type calcium channel currents in cardiac cells. *Science.* 268:1042–1045.

Mager, D.E., E. Kobrinsky, A. Masoudieh, A. Maltsev, D.R. Abernethy, and N.M. Soldatov. 2007. Analysis of functional signaling domains from fluorescence imaging and the two-dimensional continuous wavelet transform. *Biophys. J.* 93:2900–2910.

Mains, R.E., and P.H. Patterson. 1973. Primary cultures of dissociated sympathetic neurons. I. Establishment of long-term growth in culture and studies of differentiated properties. *J. Cell Biol.* 59:329–345.

Mintz, I.M., B.L. Sabatini, and W.G. Regehr. 1995. Calcium control of transmitter release at a cerebellar synapse. *Neuron.* 15:675–688.

Morgan, J.I., and T. Curran. 1986. Role of ion flux in the control of c-fos expression. *Nature.* 322:552–555.

Mori, M.X., M.G. Erickson, and D.T. Yue. 2004. Functional stoichiometry and local enrichment of calmodulin interacting with Ca2+ channels. *Science.* 304:432–435.

Murata, Y., H. Iwasaki, M. Sasaki, K. Inaba, and Y. Okamura. 2005. Phosphoinositide phosphatase activity coupled to an intrinsic voltage sensor. *Nature.* 435:1239–1243.

Murphy, T.H., P.F. Worley, and J.M. Baraban. 1991. L-type voltage-sensitive calcium channels mediate synaptic activation of immediate early genes. *Neuron.* 7:625–635.

O'Lague, P.H., K. Obata, P. Claude, E.J. Furshpan, and D.D. Potter. 1974. Evidence for cholinergic synapses between dissociated rat sympathetic neurons in cell culture. *Proc. Natl. Acad. Sci. USA.* 71:3602–3606.

O'Lague, P.H., E.J. Furshpan, and D.D. Potter. 1978. Studies on rat sympathetic neurons developing in cell culture. II. Synaptic mechanisms. *Dev. Biol.* 67:404–423.

Pietrobon, D., and P. Hess. 1990. Novel mechanism of voltage-dependent gating in L-type calcium channels. *Nature.* 346:651–655.

Pitt, G.S., R.D. Zuhlke, A. Hudmon, H. Schulman, H. Reuter, and R.W. Tsien. 2001. Molecular basis of calmodulin tethering and Ca2+-dependent inactivation of L-type Ca2+ channels. *J. Biol. Chem.* 276:30794–30802.

Rios, E., and G. Brum. 1987. Involvement of dihydropyridine receptors in excitation-contraction coupling in skeletal muscle. *Nature.* 325:717–720.

Sakagami, H., A. Kamata, H. Nishimura, J. Kasahara, Y. Owada, Y. Takeuchi, M. Watanabe, K. Fukunaga, and H. Kondo. 2005. Prominent expression and activity-dependent nuclear translocation of Ca2+/calmodulin-dependent protein kinase Idelta in hippocampal neurons. *Eur. J. Neurosci.* 22:2697–2707.

Santana, L.F., H. Cheng, A.M. Gomez, M.B. Cannell, and W.J. Lederer. 1996. Relation between the sarcolemmal Ca2+ current and Ca2+ sparks and local control theories for cardiac excitation-contraction coupling. *Circ. Res.* 78:166–171.

Sather, W.A., and E.W. McCleskey. 2003. Permeation and selectivity in calcium channels. *Annu. Rev. Physiol.* 65:133–159.

Schneggenburger, R., and E. Neher. 2000. Intracellular calcium dependence of transmitter release rates at a fast central synapse. *Nature.* 406:889–893.

Schneggenburger, R., and E. Neher. 2005. Presynaptic calcium and control of vesicle fusion. *Curr. Opin. Neurobiol.* 15:266–274.

Schneider, M.F. 1994. Control of calcium release in functioning skeletal muscle fibers. *Annu. Rev. Physiol.* 56:463–484.

Schneider, M.F., and W.K. Chandler. 1973. Voltage dependent charge movement of skeletal muscle: a possible step in excitation-contraction coupling. *Nature.* 242:244–246.

Shahrezaei, V., A. Cao, and K.R. Delaney. 2006. Ca2+ from one or two channels controls fusion of a single vesicle at the frog neuromuscular junction. *J. Neurosci.* 26:13240–13249.

Simon, S.M., and R.R. Llinas. 1985. Compartmentalization of the submembrane calcium activity during calcium influx and its significance in transmitter release. *Biophys. J.* 48:485–498.

Soderling, T.R. 1999. The Ca-calmodulin-dependent protein kinase cascade. *Trends Biochem. Sci.* 24:232–236.

Stern, M.D. 1992. Theory of excitation-contraction coupling in cardiac muscle. *Biophys. J.* 63:497–517.

Sternberg, S. 1983. Biomedical image processing. *Computer.* 16:22–34.

Sudhof, T.C. 2004. The synaptic vesicle cycle. *Annu. Rev. Neurosci.* 27:509–547.

Sugita, R., H. Mochizuki, T. Ito, H. Yokokura, R. Kobayashi, and H. Hidaka. 1994. Ca2+/calmodulin-dependent protein kinase kinase cascade. *Biochem. Biophys. Res. Commun.* 203:694–701.

Takeda, H., Y. Kitaoka, Y. Hayashi, T. Kumai, Y. Munemasa, H. Fujino, S. Kobayashi, and S. Ueno. 2007. Calcium/calmodulin-dependent protein kinase II regulates the phosphorylation of CREB in NMDA-induced retinal neurotoxicity. *Brain Res.* 1184:306–315.

Thiagarajan, T.C., E.S. Piedras-Renteria, and R.W. Tsien. 2002. alpha- and betaCaMKII. Inverse regulation by neuronal activity and opposing effects on synaptic strength. *Neuron.* 36:1103–1114.

Vizard, T.N., G.W. O'Keeffe, H. Gutierrez, C.H. Kos, D. Riccardi, and A.M. Davies. 2008. Regulation of axonal and dendritic growth by the extracellular calcium-sensing receptor. *Nat. Neurosci.* 11:285–291.

Wakamori, M., M. Strobeck, T. Niidome, T. Teramoto, K. Imoto, and Y. Mori. 1998. Functional characterization of ion permeation pathway in the N-type Ca2+ channel. *J. Neurophysiol.* 79:622–634.

Wang, S.Q., L.S. Song, E.G. Lakatta, and H. Cheng. 2001. Ca2+ signalling between single L-type Ca2+ channels and ryanodine receptors in heart cells. *Nature.* 410:592–596.

Weick, J.P., R.D. Groth, A.L. Isaksen, and P.G. Mermelstein. 2003. Interactions with PDZ proteins are required for L-type calcium channels to activate cAMP response element-binding protein-dependent gene expression. *J. Neurosci.* 23:3446–3456.

West, A.E., E.C. Griffith, and M.E. Greenberg. 2002. Regulation of transcription factors by neuronal activity. *Nat. Rev. Neurosci.* 3:921–931.

Wheeler, D.G., and E. Cooper. 2001. Depolarization strongly induces human cytomegalovirus major immediate-early promoter/enhancer activity in neurons. *J. Biol. Chem.* 276:31978–31985.

Wheeler, D.G., C.F. Barrett, and R.W. Tsien. 2006. L-type calcium channel ligands block nicotine-induced signaling to CREB by inhibiting nicotinic receptors. *Neuropharmacology*. 51:27–36.

Wiznerowicz, M., and D. Trono. 2003. Conditional suppression of cellular genes: lentivirus vector-mediated drug-inducible RNA interference. *J. Virol.* 77:8957–8961.

Wu, L.G., and P. Saggau. 1994. Presynaptic calcium is increased during normal synaptic transmission and paired-pulse facilitation, but not in long-term potentiation in area CA1 of hippocampus. *J. Neurosci.* 14:645–654.

Xiao, R.P., H. Cheng, W.J. Lederer, T. Suzuki, and E.G. Lakatta. 1994. Dual regulation of Ca2+/calmodulin-dependent kinase II activity by membrane voltage and by calcium influx. *Proc. Natl. Acad. Sci. USA.* 91:9659–9663.

Xu, W., and D. Lipscombe. 2001. Neuronal Ca(V)1.3alpha(1) L-type channels activate at relatively hyperpolarized membrane potentials and are incompletely inhibited by dihydropyridines. *J. Neurosci.* 21:5944–5951.

Yang, J., P.T. Ellinor, W.A. Sather, J.F. Zhang, and R.W. Tsien. 1993. Molecular determinants of Ca2+ selectivity and ion permeation in L-type Ca2+ channels. *Nature.* 366:158–161.

Yuan, W., and D.M. Bers. 1994. Ca-dependent facilitation of cardiac Ca current is due to Ca-calmodulin-dependent protein kinase. *Am. J. Physiol.* 267:H982–H993.

Zhang, H., A. Maximov, Y. Fu, F. Xu, T.S. Tang, T. Tkatch, D.J. Surmeier, and I. Bezprozvanny. 2005. Association of CaV1.3 L-type calcium channels with Shank. *J. Neurosci.* 25:1037–1049.

Zhao, R., L. Liu, and A.R. Rittenhouse. 2007. Ca2+ influx through both L- and N-type Ca2+ channels increases c-fos expression by electrical stimulation of sympathetic neurons. *Eur. J. Neurosci.* 25:1127–1135.

Zuhlke, R.D., G.S. Pitt, K. Deisseroth, R.W. Tsien, and H. Reuter. 1999. Calmodulin supports both inactivation and facilitation of L-type calcium channels. *Nature.* 399:159–162.